

## Biennial report for Permanent Supersite/Natural Laboratory

### *Virunga Volcanoes Supersite: 2017- 2019*

Status	Permanent Supersite
History	<a href="http://geo-gsnl.org/supersites/permanent-supersites/virunga-supersite/">http://geo-gsnl.org/supersites/permanent-supersites/virunga-supersite/</a>
Supersite Coordinator	<p><b>Charles Balagizi</b></p> <p><i>Goma Volcano Observatory</i></p> <p><i>142, Avenue du Rond-Point,</i></p> <p><i>Quartier des Volcans,</i></p> <p><i>Goma City, Democratic Republic of the Congo</i></p> <p>Email: <a href="mailto:balagizi.charles@gmail.com">balagizi.charles@gmail.com</a></p> <p><a href="tel:+243975803568">Cell : +243 975803568</a></p>

## 1. Abstract

The Virunga Volcanoes is the first Supersite established on the African continent in a highly populated Multi-hazards region. This permanent Supersite was established in a critical context as little was known about the Virunga hazards sources and their dynamics, and little done as measures to evaluate, mitigate and reduce their impacts. Similarly, the active volcanoes are poorly studied and monitored, because of the lack of both qualified human resources and appropriate infrastructures. Therefore, the establishment of the “Virunga Volcanoes Supersite” aimed mostly at helping put together local and international scientists and agencies; support them to access to Earth Observatory (EO) data and potentially to equipment for ground-based data collection, as well as the building of a pool of collaboration. The expectation was that the above-mentioned collaborations and supports would improve the early warning capacity of the local scientists and agencies involved in Natural Hazards Assessment and volcano monitoring, risk reduction and management.

After two years of existence, the Virunga Volcanoes Supersite has allowed the building of institutional collaboration between the Goma Volcano Observatory and some of the world leading institutes specialized in the study and monitoring of active volcanoes, and the assessment of related hazards (e.g. Italian INGV, United States USGS-VDAP, discussions are ongoing for others). The supersite has also allowed the access-free of charge- to a variety of EO data, e.g. COSMO-SkyMed SAR data from the Agenzia Spaziale Italiana, Pleiades from the Centre National d’Etudes Spaciales. More importantly, the Virunga Volcanoes Supersite has brought a large number of local and international scientists and agencies work together to and study Nyiragongo and Nyamulagira active volcanoes in order to better understand their eruptive mechanism, and hence better assess the related hazards and manage risks. Through this pool of collaboration, numerous activities have been successfully conducted, going from field works to assistance ordering and processing EO data, which yielded the production of useful hazards maps. Thus, the Virunga has requested and successfully obtained the activation of the Copernicus EMS services for the Virunga volcanoes for risk analyses with a focus on volcanic hazard. The later has yielded the production of hazards maps for future eruptions management, the collection of ground-based data used to produce Risk and Recovery mapping of Virunga volcanoes, as well as the production of thorough natural hazards assessment in the Virunga region and Lake Kivu. However, similar works have to be conducted in other parts of the Area of Interest of the Virunga Volcanoes Supersite, and hence the future works that use EO data (InSAR and Pleiades, principally) will aim at (1) continuing the ongoing study and monitoring of ground deformation of Nyiragongo and Nyamulagira volcanoes; (2) mapping and monitoring earthquakes and earthquake-triggered landslides in Lake Kivu Basin; (3) mapping of normal and non-normal faults in the Lake Kivu Basin, (4) along with geohazards assessment and forecast in Virunga and Lake Kivu Basin regions

Most of these results were obtained while the Virunga Volcanoes Supersite has any budget, as they were conducted through voluntary international partnership, as are all the GEO Geohazard Supersites and Natural Laboratory initiative (GSNL). On the other hand, this prevented the Virunga Supersite from realizing some key activities such as long-term trainings abroad or



acquiring infrastructures and equipment useful for ground-based data collection, and data processing in general. However, some of the activities that required funding have benefited from the support from INGV, the USGS-VDAP, the Volcano Active foundation, the International Association of Volcanology and Chemistry of the Earth's Interior (IAVCEI) which for instance supported short trainings, the donation of some equipment for some ground-based data collection, the processing of EO data and the attendance to meetings and workshops. Therefore, the Virunga Volcanoes Supersite is lacking of funds to support its mid to long-term objectives which are to permit local scientists access the strong trainings, skills and experience for both ground based and EO data continuous acquisition and analysis for volcano monitoring, to continuously assess natural hazards, vulnerability and risks in the region and regularly produce the related updated maps.

## 2. Scientists/science teams

<b>Charles M. Balagizi</b>	Geochemistry and Environmental Department, Goma Volcano Observatory. 142, Avenue du Rond-Point, Quartier des Volcans, Goma City, Democratic Republic of the Congo <a href="mailto:balagizi.charles@gmail.com">balagizi.charles@gmail.com</a> <a href="https://www.researchgate.net/profile/Charles_Balagizi">https://www.researchgate.net/profile/Charles_Balagizi</a>
<b>Georges Mavonga</b>	Department of Seismology, Goma Volcano Observatory 142, Avenue du Rond-Point, Quartier des Volcans, Goma City, Democratic Republic of the Congo <a href="mailto:mavotulu@gmail.com">mavotulu@gmail.com</a>
<b>Celestin Kasereka</b>	Goma Volcano Observatory, Democratic Republic of the Congo <a href="mailto:mahindageophys@gmail.com">mahindageophys@gmail.com</a>
<b>Honoré Ciraba</b>	Goma Volcano Observatory, Democratic Republic of the Congo <a href="mailto:honoreciraba@yahoo.fr">honoreciraba@yahoo.fr</a>
<b>Katcho Karume</b>	Goma Volcano Observatory, Democratic Republic of the Congo <a href="mailto:kkatcho@yahoo.com">kkatcho@yahoo.com</a>
<b>Mathieu Yalire</b>	Goma Volcano Observatory, Democratic Republic of the Congo <a href="mailto:yaliremat@yahoo.fr">yaliremat@yahoo.fr</a>
<b>Mukambilwa Cibuya</b>	Goma Volcano Observatory, Democratic Republic of the Congo <a href="mailto:kmuka1@yahoo.fr">kmuka1@yahoo.fr</a>
<b>Albert Kyambikwa</b>	Goma Volcano Observatory, Democratic Republic of the Congo <a href="mailto:albertuskabi@gmail.com">albertuskabi@gmail.com</a>
<b>Niche Mashagi</b>	Goma Volcano Observatory, Democratic Republic of the Congo <a href="mailto:nichemashagi@gmail.com">nichemashagi@gmail.com</a>
<b>Marcellin Kasereka</b>	Goma Volcano Observatory, Democratic Republic of the Congo <a href="mailto:marcellinkasereka16@gmail.com">marcellinkasereka16@gmail.com</a>
<b>Jeanpy Lukindula</b>	Goma Volcano Observatory, Democratic Republic of the Congo <a href="mailto:jeanpywilondja@gmail.com">jeanpywilondja@gmail.com</a>
<b>Bo Galle</b>	Chalmers University of Technology, Hörsalsvägen 11, Floor 4 <a href="mailto:bo.galle@chalmers.se">bo.galle@chalmers.se</a> <a href="http://www.chalmers.se/en/Pages/default.aspx">http://www.chalmers.se/en/Pages/default.aspx</a>

<b>Michael Poland</b>	U.S. Geological Survey, Cascades Volcano Observatory 1300 SE Cardinal Court, Suite 100 Vancouver, WA 98683 <a href="mailto:mpoland@usgs.gov">mpoland@usgs.gov</a> <a href="https://www.usgs.gov/staff-profiles/michael-poland">https://www.usgs.gov/staff-profiles/michael-poland</a>
<b>Marcello Liotta</b>	Istituto Nazionale di Geofisica e Vulcanologia Via Ugo La Malfa, 153 90146 - Palermo (Italy) <a href="mailto:marcello.liotta@ingv.it">marcello.liotta@ingv.it</a> <a href="https://sites.google.com/ingv.it/marcello-liotta/">https://sites.google.com/ingv.it/marcello-liotta/</a>
<b>Yosuke Aoki</b>	Earthquake Research Institute, University of Tokyo 1-1 Yayoi 1, Bunkyo-ku- Tokyo 113-0032, Japan <a href="mailto:yaoki@eri.u-tokyo.ac.jp">yaoki@eri.u-tokyo.ac.jp</a> <a href="http://www.eri.u-tokyo.ac.jp">http://www.eri.u-tokyo.ac.jp</a>
<b>Mariarosaria Manzo</b>	Istituto per il Rilevamento Elettromagnetico dell'Ambiente (IREA), Consiglio Nazionale delle Ricerche (CNR), Via Diocleziano 328, 80124 Napoli, Italy, <a href="mailto:manzo.mr@irea.cnr.it">manzo.mr@irea.cnr.it</a>
<b>Riccardo Lanari</b>	Istituto per il Rilevamento Elettromagnetico dell'Ambiente (IREA), Consiglio Nazionale delle Ricerche (CNR), Via Diocleziano 328, 80124 Napoli, Italy, <a href="mailto:lanari.r@irea.cnr.it">lanari.r@irea.cnr.it</a>
<b>Manuela Bonano</b>	Istituto per il Rilevamento Elettromagnetico dell'Ambiente (IREA), Consiglio Nazionale delle Ricerche (CNR), Via Diocleziano 328, 80124 Napoli, Italy, <a href="mailto:bonano.m@irea.cnr.it">bonano.m@irea.cnr.it</a>
<b>Claudio De Luca</b>	Istituto per il Rilevamento Elettromagnetico dell'Ambiente (IREA), Consiglio Nazionale delle Ricerche (CNR), Via Diocleziano 328, 80124 Napoli, Italy, <a href="mailto:deluca.c@irea.cnr.it">deluca.c@irea.cnr.it</a>
<b>Giovanni Onorato</b>	Istituto per il Rilevamento Elettromagnetico dell'Ambiente (IREA), Consiglio Nazionale delle Ricerche (CNR), Via Diocleziano 328, 80124 Napoli, Italy, <a href="mailto:onorato.g@irea.cnr.it">onorato.g@irea.cnr.it</a>
<b>Gaetana Ganci</b>	Istituto Nazionale di Geofisica e Vulcanologia Piazza Roma, 2 - 95125 Catania <a href="mailto:gaetana.ganci@ingv.it">gaetana.ganci@ingv.it</a>
<b>Ciro Del Negro</b>	Istituto Nazionale di Geofisica e Vulcanologia Piazza Roma, 2 - 95125 Catania <a href="mailto:ciro.delnegro@ingv.it">ciro.delnegro@ingv.it</a>
<b>Annalisa Cappello</b>	Istituto Nazionale di Geofisica e Vulcanologia Piazza Roma, 2 - 95125 Catania <a href="mailto:annalisa.cappello@ingv.it">annalisa.cappello@ingv.it</a>
<b>Diego Coppola</b>	Dipartimento di Scienze della Terra, Università degli Studi di Torino TORINO, Italia <a href="mailto:diego.coppola@unito.it">diego.coppola@unito.it</a>
<b>Jake Lowenstern</b>	Volcano Disaster Assistance Program, USGS Cascades Volcano Observatory 1300 SE Cardinal Court; Vancouver, WA 98683-USA <a href="mailto:jlownstn@usgs.gov">jlownstn@usgs.gov</a>
<b>Peter Kelly</b>	Volcano Disaster Assistance Program, USGS Cascades Volcano Observatory 1300 SE Cardinal Court; Vancouver, WA 98683-USA <a href="mailto:pkelly@usgs.gov">pkelly@usgs.gov</a>
<b>Wendy McCausland</b>	Volcano Disaster Assistance Program, USGS Cascades Volcano Observatory 1300 SE Cardinal Court; Vancouver, WA 98683-USA

	<a href="mailto:wmccausland@usgs.gov">wmccausland@usgs.gov</a>
<b>Raymond J. Durrheim</b>	School of Geosciences University of the Witwatersrand Johannesburg, South Africa <a href="mailto:Raymond.Durrheim@wits.ac.za">Raymond.Durrheim@wits.ac.za</a>
<b>Antoine Kies</b>	University of Luxembourg <a href="mailto:antoine.kies@uni.lu">antoine.kies@uni.lu</a>
<b>Sven Borgstrom</b>	Istituto Nazionale di Geofisica e Vulcanologia, Vesuviano Observatory, Italia <a href="mailto:sven.borgstrom@ingv.it">sven.borgstrom@ingv.it</a>
<b>Mauro Coltelli</b>	Istituto Nazionale di Geofisica e Vulcanologia Piazza Roma, 2 - 95125 Catania-Italia <a href="mailto:mauro.coltelli@ingv.it">mauro.coltelli@ingv.it</a>
<b>Mario Mattia</b>	Istituto Nazionale di Geofisica e Vulcanologia Piazza Roma, 2 - 95125 Catania-Italia <a href="mailto:mario.mattia@ingv.it">mario.mattia@ingv.it</a>
<b>Patrick Allard</b>	Institut de Physique de Paris <a href="mailto:pallard@ipgp.fr">pallard@ipgp.fr</a>

### Scientists/science teams issues

*The Virunga Volcanoes Supersite benefited from the support of more than 25 international scientists when the proposal was put forward to request from the COES the establishment of a supersite on Virunga. Since then, the team has grown up with new adhesion of many other members, mostly composed of local scientists.*

*The ones listed in the above table are those who were actively involved in the data processing and collaborated in the field data collection to produce some of the results listed in the below sections, particularly in the presently published papers that used ground-based, the request and processing of EO data.*

*Hence, few local scientists had the chance to access the data because of the present major issue related to the data sharing among the scientists, the lack of infrastructures (e.g. proper computer machines and software to process the data), the lack of access to the internet for EO data download and processing, and for some the lack of proper training to process the data. In some cases, the EO data were downloaded in Europe and sent to the Virunga using hard drivers, but this could be possible only for data to be used for training which up to now is mostly done through emails exchange, particularly with regards to EO data.*

## 3. In situ data

Type of data	Data provider	How to access	Type of access
Seismic	Goma Volcano Observatory (GVO)	Published papers* Contact GVO**	Unregistered Public
GPS	GVO	Contact GVO**	GSNL scientists

<b>Gas measurements</b>	GVO	<i>Published papers*</i>	<i>Unregistered Public GSNL scientists</i>
<b>Surface waters chemistry</b>	GVO	<i>Published papers* Contact GVO**</i>	<i>Unregistered Public GSNL scientists</i>
<b>Rainwater chemistry</b>	GVO	<i>Published papers* Contact GVO**</i>	<i>Unregistered Public GSNL scientists</i>

*\*Published data are freely accessible; the Goma Volcano Observatory may be contacted for guidance in case of issues*

*\*\*Archived unpublished data or recently collected data are available on request, and based on the data policy for data sharing and management among the Virunga Supersite scientific community.*

### **In situ data issues**

Most of the existing in situ data are collected in partnership with international collaborators. The data collection activities started before the Virunga was made a permanent Supersite, and hence any possibilities of in situ data sharing with other scientists was not included in the agreements signed between the Goma Volcano Observatory and its partners. This is the reason why the Virunga Volcanoes Supersite coordinator with the help of his Core Team prepared a Data Policy that was proposed to the GVO's staff, and after amendment it was approved and now known as "The Virunga Volcanoes Supersite Partnership and Data Policy" and is now available at the GSNL website [http://geo-gsnl.org/wp-content/Documents/Supersites/Virunga/History/Virunga%20Supersite\\_Data%20Policy.pdf](http://geo-gsnl.org/wp-content/Documents/Supersites/Virunga/History/Virunga%20Supersite_Data%20Policy.pdf)

According to this data policy, the ground-based data and results should be made available for full and open access after publication or in any case within 2 years ("embargo period") since their collection/generation. During the embargo period the data/results will only be available to the owner and to his co-authors, while the relative metadata will be openly available, so that the community is aware of the data/result existence. Once the embargo period has expired, the data and metadata will be put openly available for all. However, even during the embargo period, the data/result owner is required to share its data with the GVO (local and international expert could thus access the data) for urgent monitoring purposes, during eruption or unrest events, or for specific capacity building/training activities. Before sharing, the owner can protect his authorship by assigning a DOI and one of the recommended data. The remaining issue is related to the fact that lack of infrastructures at local level to host the data, and make them accessible through a given portal.

Because there is still a strong need to enlarge and improve the existing in situ data collection networks and activities, the Virunga Supersite is searching equipment to deploy in the field to reach this key goal in order to allow scientists access as large as possible data to better understand the volcanoes eruptive mechanism, and for improved monitoring strategies and hazards assessment. As an example, a recently published paper (Mavonga et al., 2019; <https://doi.org/10.1007/s00024-018-2084-6>) on Seismic Hazard Assessment for the Virunga strongly recommended the installation of new seismic stations, i.e. strengthening of existing seismic networks, to improve the produced ground motion prediction models and hazards

maps. Moreover, many geophysical fields are still none explored yet in the Virunga, of which the data could be of great importance for the interpretation of the ones presently collected, or for bringing new insights into our present understanding of Virunga Volcanoes and the hazards.

## 4. Satellite data

Type of data	Data provider	How to access	Type of access
<b>COSMO-SkyMed</b>	ASI	POC requests access from ASI for GSNL scientists individual users, data then accessible via <a href="#">UNAVCO</a>	GSNL scientists
<b>Pleiades</b>	CNES	POC requests access from CNES for individual users	GSNL scientists
<b>Sentinel-1 a/b</b>	ESA	<a href="https://scihub.copernicus.eu/">https://scihub.copernicus.eu/</a>	Registered public
<b>ASTER EO-1 (Hyperion) MODIS</b>	NASA	<a href="https://terra.nasa.gov/about/terra-instruments/modis">https://terra.nasa.gov/about/terra-instruments/modis</a>  <a href="https://modis.gsfc.nasa.gov/">https://modis.gsfc.nasa.gov/</a>	Registered public
<b>Landsat</b>	USGS	<a href="https://www.usgs.gov/land-resources/nli/landsat/landsat-data-access?qt-science_support_page_related_con=0#qt-science_support_page_related_con">https://www.usgs.gov/land-resources/nli/landsat/landsat-data-access?qt-science_support_page_related_con=0#qt-science_support_page_related_con</a>	Registered public
<b>AVHRR</b>	NOAA	<a href="https://earth.esa.int/web/guest/missions/3rd-party-missions/current-missions/noaa-avhrr">https://earth.esa.int/web/guest/missions/3rd-party-missions/current-missions/noaa-avhrr</a>	Registered public

### Satellite data issues

#### ➤ COSMO-SkyMed SAR datasets

ASI satellite data policy requires users to be sponsored by the PoC and then to submit contact information and a brief research plan, which is reviewed before approval. The submitted proposal aimed to collect the largest X-band COSMO-SkyMed SAR datasets over the Virunga region, since they are extremely important to monitor deformation processes in the Nyiragongo and Nyamulagira volcanoes starting from 2009, thus enhancing the scientific understanding of rift-zone volcanism and also forecasting the temporal and spatial extent of the next possible eruptions.

After proposal acceptance, the interaction with ASI concerning the provision of archive COSMO-SkyMed data has been very good. Handling and use of such satellite data have been in agreement with guidelines provided by ASI. In particular, one descending and one ascending COSMO-SkyMed Stripmap archive datasets (April 2011-February 2019) have been collected and processed. New planned acquisitions, programmed over some areas closer to Lake Kivu Basin (for earthquakes and earthquake-triggered landslides mapping and monitoring), have not been collected yet.

We also benefitted from the availability of data acquired from the C-band Sentinel-1 (S-1) constellation of the European Copernicus Programme (TOPS mode) over the Virunga region

(descending orbits along the June 2016- October 2019 time interval). The selected Sentinel-1 data include the same geographical area covered by the COSMO-SkyMed dataset, even though with a spatial extent of about 250 x 250 km<sup>2</sup>, which allows us to identify a larger portion of the volcanic rift movement. Note that the European Commission data policy for S-1 data is free and open access, so the users can easily access the S-1 archive through the Scientific Hub that only requires a public registration process.

### ➤ Pleiades images

According to Pleiades images in the Virunga region, one of the biggest issues is the possibility to find acquisitions with a minimum percentage of clouds. The acquisition plan started in December 2018 and, in spite of this, the two volcanic areas Nyiragongo and Nyamuragira, are still not covered. The redundancy of acquisitions in the same region is the only means to obtain the complete coverage. The programming period was extended until August 31<sup>st</sup> 2020, so we hope to cover the missing areas in the next few months.

From a technical point of view, many Pleiades scenes are split into smaller tiles for size management, while a unique Rational Polynomial Coefficient (RPC) file is provided for the scene. This is not easily handled by the MicMac software. Indeed MicMac requires an RPC file for each image. In order to deal with this aspect, we merged the tiles into a single file and then process it with MicMac. In this way we solved the problem, but the processing is very time consuming.

## 5. Research results

### 5.1. In situ Data

#### 5.1.1. Seismic Hazard Assessment of the Democratic Republic of Congo and Environs Based on the GEM–SSA Catalogue and a New Seismic Source Model

A new probabilistic seismic hazard assessment has been performed for the Democratic Republic of Congo (DRC) and surrounding areas in general, and the Virunga region in particular. The DRC encompasses both intra-plate and active tectonic areas associated with the Congo Craton and the western branch of the East African Rift System, respectively (Figure 1A, and Table 1 for further details). The seismic hazard assessment is based on the new Sub-Saharan-Global Earthquake Model Sub-Saharan-Global Earthquake Model earthquake catalogue with homogeneous magnitude representation (M<sub>w</sub>) created by augmenting available global catalogues (e.g. International Seismological Center (ISC)-Reviewed, ISC–GEM, GCMT) with information from local agencies and regional projects, particularly from the Africa Array network. This catalogue spans from 1900 to 2015. The initial declustered catalogue has 782 events (Figure 1B). The historical earthquake record is sparse with significant variation in completeness over time across different regions. After taking the completeness of the catalogue into account, the final declustered catalogue used to calibrate the magnitude-frequency distribution of events used for the seismic hazard assessment spans 55 years (from



1960 to 2015) with 398 events and a magnitude of completeness of about 4.5. The maximum credible magnitude of earthquakes was determined using the entire catalogue from 1900 to 2015. The seismotectonic zonation into 15 seismic source areas was done on the basis of the regional geological structure, neotectonic fault systems, basin architecture and distribution of thermal springs and earthquake epicentres.

Also, consideration was given to a regional strain rate model developed for the East African Rift by Saria et al. (Journal of Geophysical Research, 119, 3584–3600, 2014) in the frame of the GEM Strain Rate Project. Tectonic information was derived mostly from the scientific literature and by integration of available datasets. The current area source model consists of a total of 15 seismic zones distributed over 6 main tectonic groups that we assume to have comparable rheological and mechanical behavior with respect to the underlying crustal geology (Figure 1C, and Table 2 for further details). The definition of these groups is essential for the regional calibration of b values. The b value is expected to be regionally stable with variations less than the uncertainty limits, while the activity rate  $\lambda$  is liable to vary substantially from one seismic source zone to another (Table 3). The Gutenberg–Richter seismic hazard parameters (Table 3) were determined using Aki's maximum likelihood method Aki (Bulletin of the Earthquake Research Institute, Tokyo University, 43, 237–239, 1965) and Weichert's method Weichert (Bulletin of the Seismological Society of America, 70, 1337–1346, 1980), and compared with extension of the Aki–Utsu b value estimator for incomplete catalogues Kijko and Smit (Bulletin of the Seismological Society of America, 102, 1183–1287, 2012). Hazard computations were performed using the Open Quake engine (version 2.7.0-1). The peak ground acceleration (PGA) and spectral acceleration at periods of 0.05, 0.1, 0.2, 0.5, 1 and 2 s was calculated using four ground motion prediction equations (GMPEs): two for active shallow crust Chiou et al. (Earthquake Spectra, 30, 1117–1153, 2014); Akkar et al. (Bulletin of Earthquake Engineering, 12, 359–387, 2014) and two for stable continental conditions Atkinson et al. (Bulletin of the Seismological Society of America, 96, 2181–2205, 2006; Pezeshk et al. (Bulletin of the Seismological Society of America, 101, 1859–1870, 2011) for soil sites corresponding to  $V_s$  30 = 600, 760 and 1500 m/s at 11 cities of the DRC and surrounding areas.



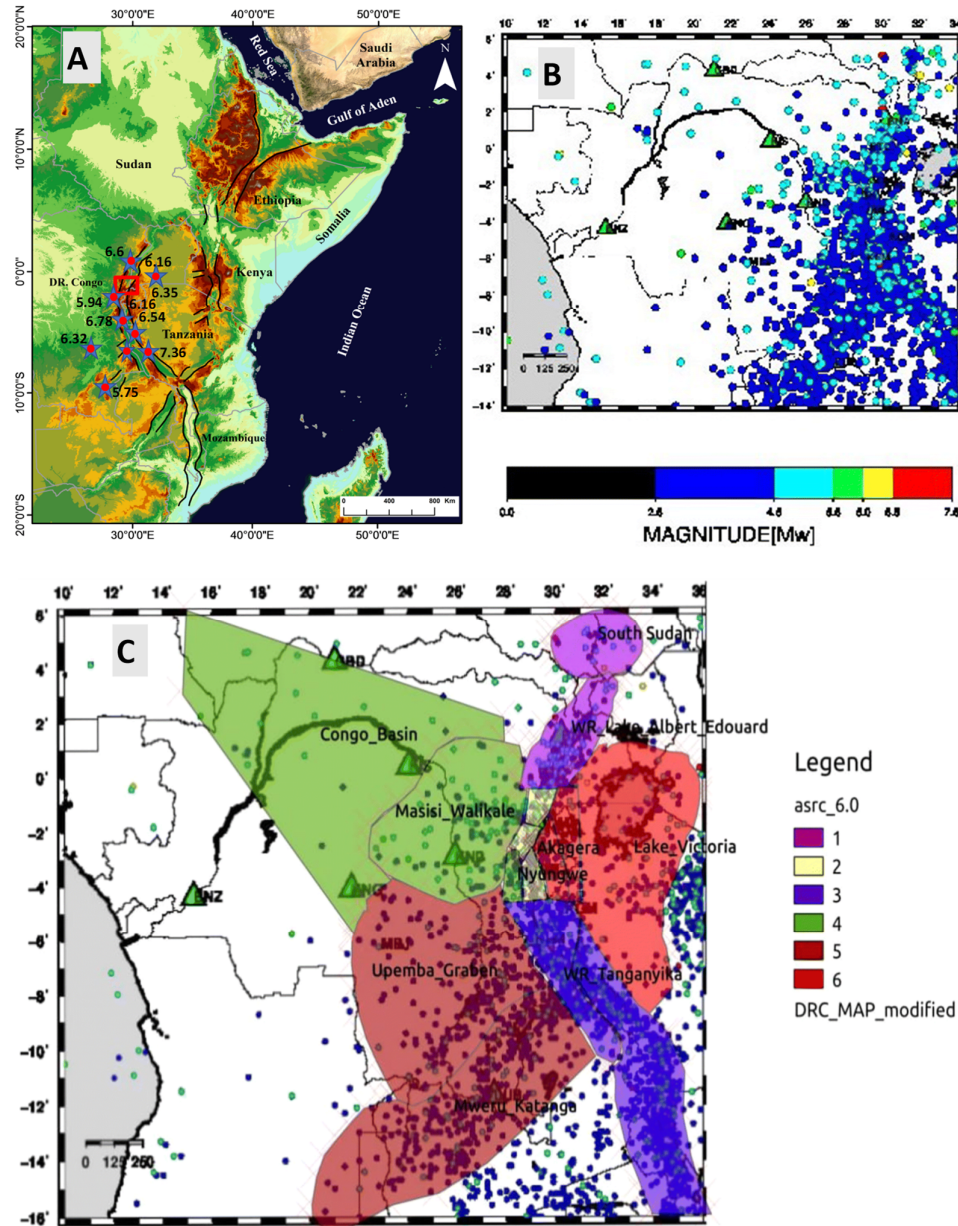


**Figure 1. (A) Map of the East Africa Rift System (EARS) and epicentres of earthquakes listed in Table 1. (B) Epicentres in the DRC and surrounding areas for the time period 1910–2015 used in the seismic hazard analysis. (C) Source zonation model used in this study (see Table 2 for details)**

The results are consistent with those obtained using the regional frequency-independent attenuation law of Mavonga (Physics of the Earth and Planetary Interiors, 62, 13–21, 2007b) developed in the Kivu Rift segment and others Twesigomwe (Journal of African Earth Sciences, 24, 183–195, 1997), and Jonathan (Some aspects of seismicity in Zimbabwe and Eastern and

Southern Africa. M.Sc. thesis. Institute of solid earth physics, Univ. Bergen, Bergen, Norway, pp. 100 (1996)), using Crisis 2012 software.

**Table 1. Earthquakes with  $M \geq 6$  in the Western Rift Valley of Africa during the past century**

Town /district (country)	Date (dd/mm/yyyy)	Magnitude (Mw)
Kasanga (Tanzania)	13/12/1910	7.36
Masaka (Uganda)	18/03/1945	6.35
Lake Moero (DRC)	5/5/1958	5.75
Uvira (DRC)	22/09/1960	6.54
Rwenzori/Toro (Uganda/DRC)	20/03/1966	6.6
Kabalo (DRC)	11/9/1992	6.32
Kisomoro (Uganda/DRC)	5/2/1994	6.16
Kalehe (DRC)	24/10/2002	6.16
Kalemie (DRC)	5/12/2005	6.78
Bukavu (DRC)	3/2/2008	5.94

**Table 2. Area sources implemented in the seismic source model for the DRC and environs**

Group ID	Source ID	Name
1	1	South Sudan
	4	Western Rift–Albertin Rift–Lake Edouard
2	5	Virunga
	6	Lake Kivu
	8	Rusizi–North Tanganyika
3	11	Western Rift–Lake Tanganyika
	12	Western Rift–Malawi–Nyassa
4	2	Congo Basin
	3	Masisi–Walikale
	7	Elila
5	14	Upemba Graben
	15	Mweru–South Katanga
6	9	Nyungwe
	10	Akagera
	13	Lake Victoria

**Table 3. Gutenberg–Richter parameters computed for the different source zones**

Group ID	Source ID	Name	Number of events	<i>b</i> value	<i>a</i> value	$\lambda$	$M_{max}$
1	1	South Sudan	24	0.92	3.579	0.275	7.59
1	4	WR_Lake_Albert_Ed.	102	0.92	4.253	1.171	7.1
2	5	Virunga	15	0.8	3.251	0.159	5.89
2	6	WR_Lake_Kivu	15	0.8	3.251	0.159	6.66
2	8	Rusizi	17	0.8	3.327	0.181	7.04
3	11	WR_Tanganyika	110	0.92	4.098	0.908	7.28
3	12	WR_Malawi-Nyassa	193	0.92	4.342	1.592	7.86
4	2	Congo Basin	15	1.29	5.02	0.164	6.38
4	3	Masisi-Walikale	71	1.29	5.695	0.776	6.46
4	7	Elila	12	1.29	4.922	0.132	5.58
6	9	Nyungwe	15	1.02	3.7	0.129	6.7
6	10	Akagera	1	1.02	2.544	0.0086	5.34
6	13	Lake_Victoria	38	1.02	4.103	0.3265	6.85
5	14	Upemba_Graben	66	0.93	3.868	0.4821	6.82
5	15	Mweru_Katanga	88	0.93	3.993	0.643	6.25

The major issue affecting the reliability of our hazard model is the lack of strong-motion recordings for the selection and validation of existing ground motion prediction models. Hence, in the study our choice of suitable GMPEs is based on the crustal structure of the EARS and the Congo and Tanzanian Cratons, relying on a set of assumptions from seismotectonic considerations that still need full validation (Figure 3). Future installation of new strong-motion stations at potentially hazardous sites and the strengthening of existing seismic networks is essential to verify the applicability of existing ground motion prediction models and to promote the development of new locally calibrated ones. For this reason, we compared the average PGA values for four cities in the Kivu Rift segment that we obtained using the Open Quake software, a logic tree with four GMPEs, and two Vs30 values (760 and 1500 m/s) with the average PGA values obtained by Delvaux et al. (2016) using the Crisis 2012 software, three regional frequency-independent attenuation relations and hard-rock site conditions. The PGA values obtained using the different approaches are remarkably consistent: Goma, 0.26 and 0.25 g; Bukavu 0.34 and 0.37 g; Bujumbura 0.30 and 0.32 g; and Kigali 0.10 and 0.17 g.

Spectral acceleration maps produced for different structural periods for 10% probability of exceedance in 50 years show that the largest accelerations are found for periods of 0.1 and 0.2 s along the western branch of the EARS (0.6–0.8 g for a structural period  $T = 0.1$  s), (Figure 2) particularly for source zones 6 and 8 in group ID 2. This is due to local soil conditions, which are likely to affect the predicted ground motion for this frequency band (5–10 Hz). This frequency range is significant from an engineering perspective, as it matches the resonance response of common buildings in urban environments. Moderate acceleration (lower than 0.2 g) is predicted further from the rift axis (Figure 2). Spectral acceleration is dependent on structural period and soil site (Figure 3). Therefore, microzonation or soil site investigations are very important for critical infrastructure. We therefore recommend that seismic hazard assessments should be improved by maintaining and expanding seismic monitoring networks,

supplementing historical and paleoseismic catalogues, and mapping active faults and the near-surface. Building codes should be formulated and enforced, and vulnerable existing buildings and infrastructure reinforced to prevent serious damage or collapse when subjected to strong shaking.

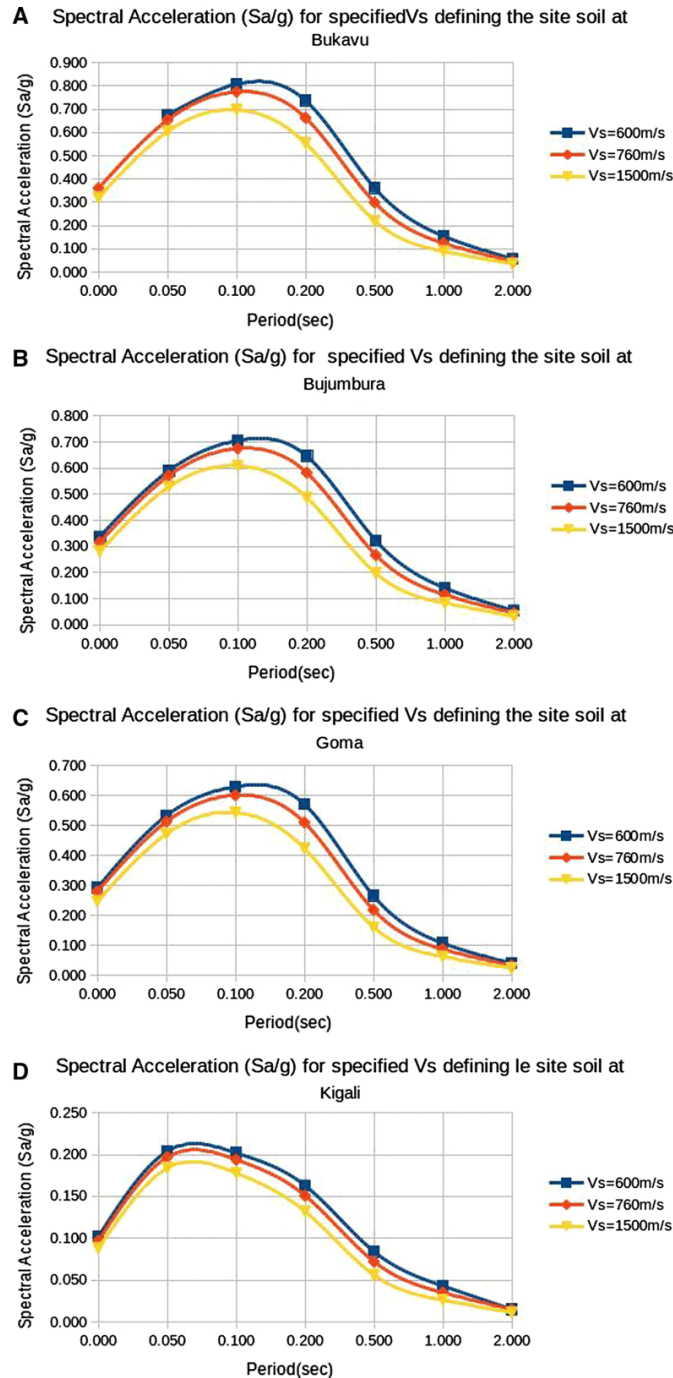


**Figure 2. (A) Mean uniform hazard spectra computed for Bukavu City. (B) Mean uniform hazard spectra computed for Bujumbura City. (C) Mean uniform hazard spectra computed for Goma City. (D) Mean uniform hazard spectra computed for Kigali City.**



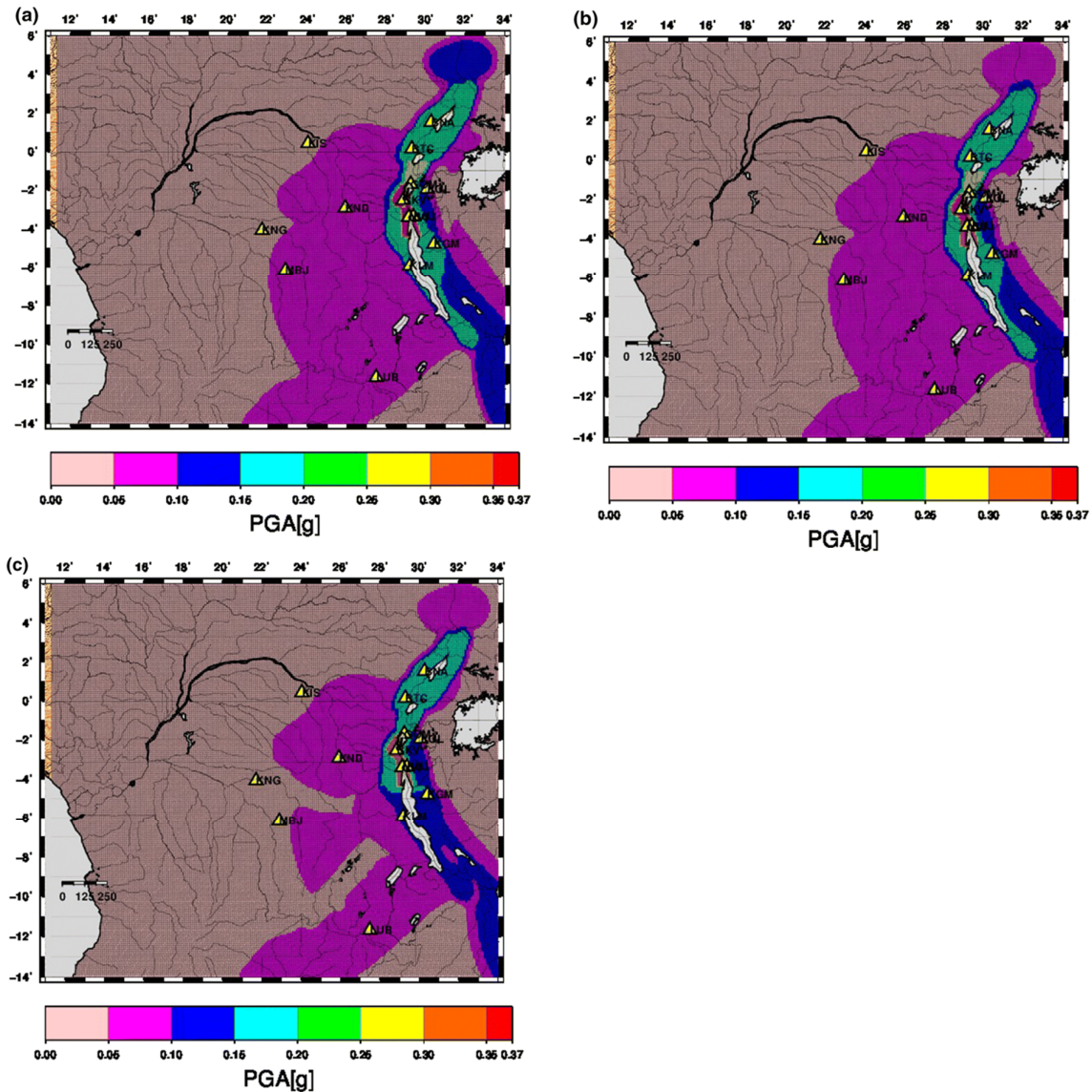


**Figure 3. (A) PGA for different soil site (Vs30) for the DRC and surrounding areas corresponding to Vs30 = 600 m/s. (B) PGA for different soil site (Vs30) for the DRC and surrounding areas corresponding to Vs30 = 760 m/s. (C) PGA for different soil site (Vs30) for the DRC and surrounding areas corresponding to Vs30 = 1500 m/s**

### 5.1.2. Natural hazards Assessment in Goma and the surrounding villages

The city of Goma and its surrounding villages are amongst the world's most densely populated regions strongly affected by volcanic hazards. In 2002 Nyiragongo volcano erupted destroying 10-15% of Goma (Figure 4) and forced a mass evacuation of the population. Hence, the ~1.5 million inhabitants of Goma and Gisenyi (Rwanda) continue to live with the threat of new lava flows and other eruptive hazards from this volcano. In the present work we mapped the network of fractures that extends from Nyiragongo summit to Goma and continues beneath Lake Kivu (Figure 4) and that gives rise to the fear that an eruption could even produce an active vent within the center of Goma or within the lake. We also discussed the hazards related to a sub-lacustrine volcanic eruption with vents in the floor of the main basin and/or Kabuno Bay of Lake Kivu and that could potentially release about 300 km<sup>3</sup> of carbon dioxide (CO<sub>2</sub>) and

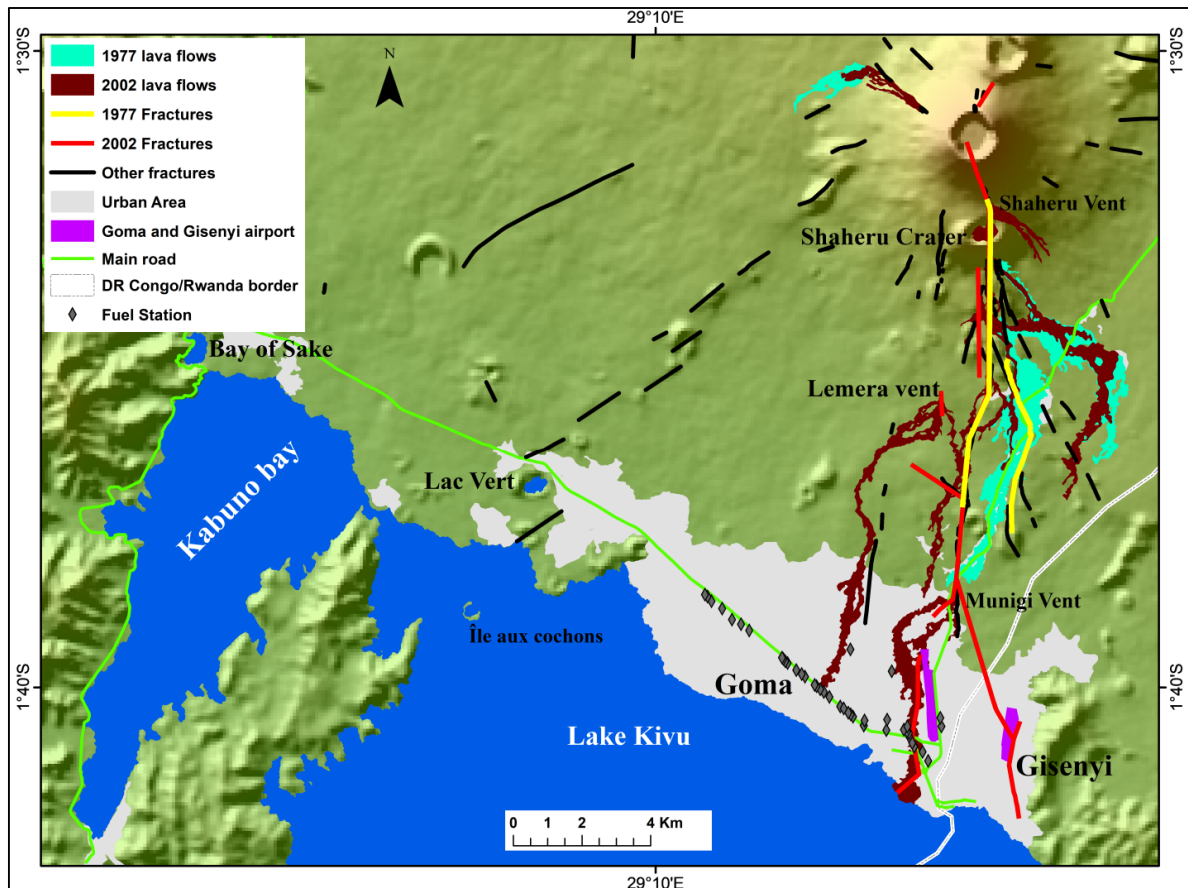


**Figure 4.** A map showing the southern flank of Nyiragongo volcano and the 1977 (yellow lines) and 2002 (red) eruptive fractures. In 2002 two lava flows reached Goma, i.e. the western flow from the Lemera vent and stopped a few meters north the main road (green line), and the eastern flow which came from the Munigi vent, blanketed part of the airport of Goma, and reached Lake Kivu. Pink dots show the fuel stations located in the lava flow pathways and along the main road in Goma

60 km<sup>3</sup> of methane (CH<sub>4</sub>) dissolved in its deep waters (Figure 5A&B), and that would be catastrophic to populations (~ 2.5 million people) along the lake shores.

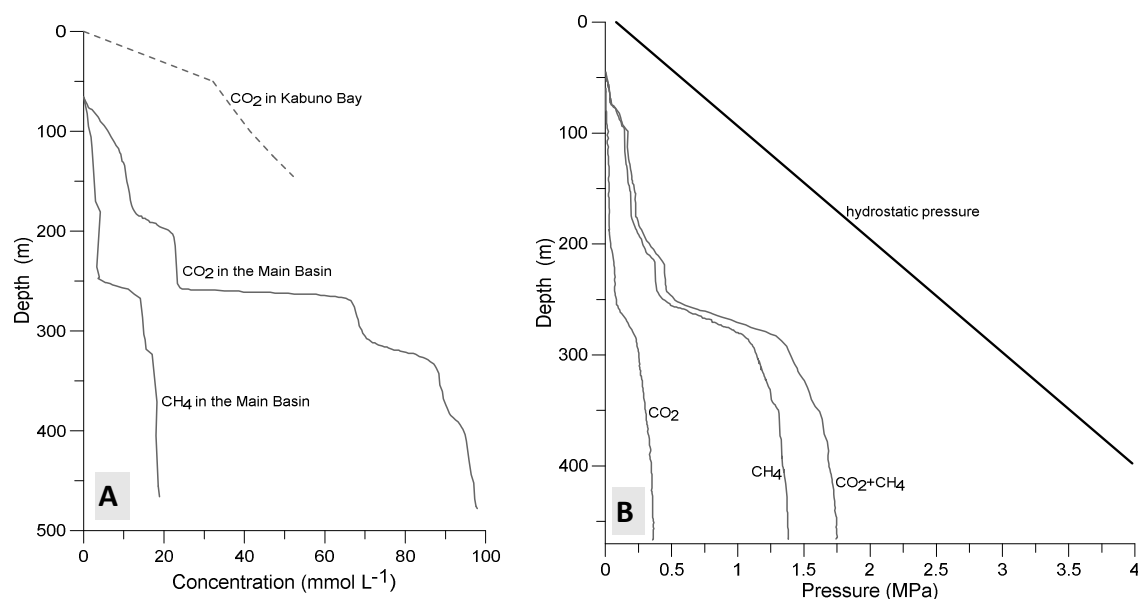


**Figure 5. CO<sub>2</sub> and CH<sub>4</sub> concentrations vertical profiles in the main basin of lake Kivu after Schmid et al. (2005); and CO<sub>2</sub> in Kabuno after Tassi et al. (2009). CO<sub>2</sub> and CH<sub>4</sub> partial pressures and total gas pressure in the main basin of Lake Kivu calculated from their concentrations (Schmid et al. 2004)**

We further inventoried the present ongoing hazards related to Nyiragongo and Nyamulagira volcanoes that silently kill people and animals, slowly destroy the environment and seriously harm the health of the population. They include Mazuku or CO<sub>2</sub>-rich locations where people often die of asphyxiation (Figure 6; together with Figure 7 that shows the CO<sub>2</sub> concentrations in some Mazuku in which the values have remained almost constant over the last 1.5 decades), the highly fluoridated surface and ground waters (Figure 8) and that cause fluorosis among population (Figure 9), and other locally neglected hazards. The volcanic gas plume causes poor air quality and acid rain, which is commonly used for drinking water (see further discussion in the section 3.1.3. on rain-plume interactions). Given the large number of people at risk and the continued movement of people to Goma and the surrounding villages, there was an urgent need for a thorough natural hazards assessment in the region. This is the reason why our work focused on the general assessment of natural hazards in the region around Goma based on field investigations, CO<sub>2</sub> measurements in Mazuku, and chemistry data for Lake Kivu, rivers and rain-water. The field investigations and the datasets are used in conjunction with extremely rich-historical (1897 to 2000) and recently published information about Nyiragongo and Nyamulagira volcanoes and Lake Kivu. We also presented maps of Mazuku and fractures in Goma, describe the volcanic eruption history with hazard assessment and mitigation implications, and consider social realities useful for an integrated risk management strategy.

Therefore, Goma and its surroundings are densely urbanized regions threatened by a variety of natural hazards. The vulnerability of inhabitants is heightened because of both the precarious living conditions and presence of many natural hazards in the region. Basic uncertainty and insecurity have made natural hazards less threatening than the problems related to daily survival. In fact, the inhabitants are more concerned about insecurity caused by war and how to obtain their daily food supply, than they are about a possible volcanic eruption, which may occur in three years, five years or more.

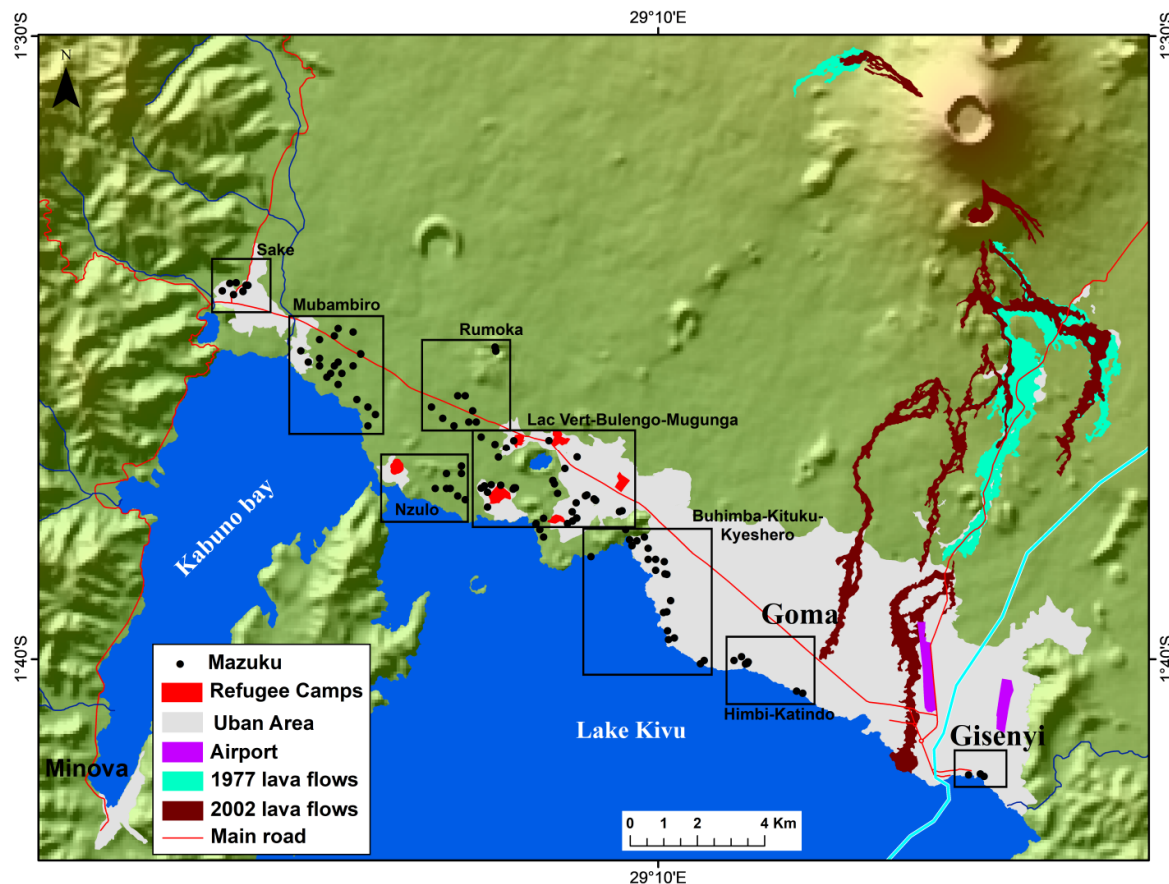


**Figure 6. Location of Mazuku in the north catchment of Lake Kivu, where concentrations range from 20 to 71% depending on location. The represented Mazuku are those that have already been investigated and inventoried by the GVO, but many others are still unknown. Priority is given to inhabited areas for risk prevention. Refugees living in camps (red dots) are the most vulnerable, but the local population remains exposed because much of their daily activities, e.g. farming and tending livestock, occur in areas containing Mazuku.**

The extension of the city limits of Goma into extremely hazardous areas and the construction of buildings on volcanic vents like that of Munigi shown in Figure 4 or in Mazuku area (Figure 6) are evidence that local population have forgotten the lesson from the Nyiragongo 2002 eruption. Proactive zoning by local authorities should prohibit building in these high-risk zones, e.g. on vent and the immediate environment, on open and active fractures in Goma (Figure 4).



In the 16 years since the last Nyiragongo eruption, the population of Goma has almost tripled. We therefore recommended that a special program educating people on volcanic and all regional hazards should be introduced into the curriculum of local educational institutions, as we estimated that more than ~70% of the current population did not experience the 2002 eruption. Hazards related to the Mazuku, gas plume, acid rain, and fluoride rich-water should be more carefully studied and integrated into local risk management plans.

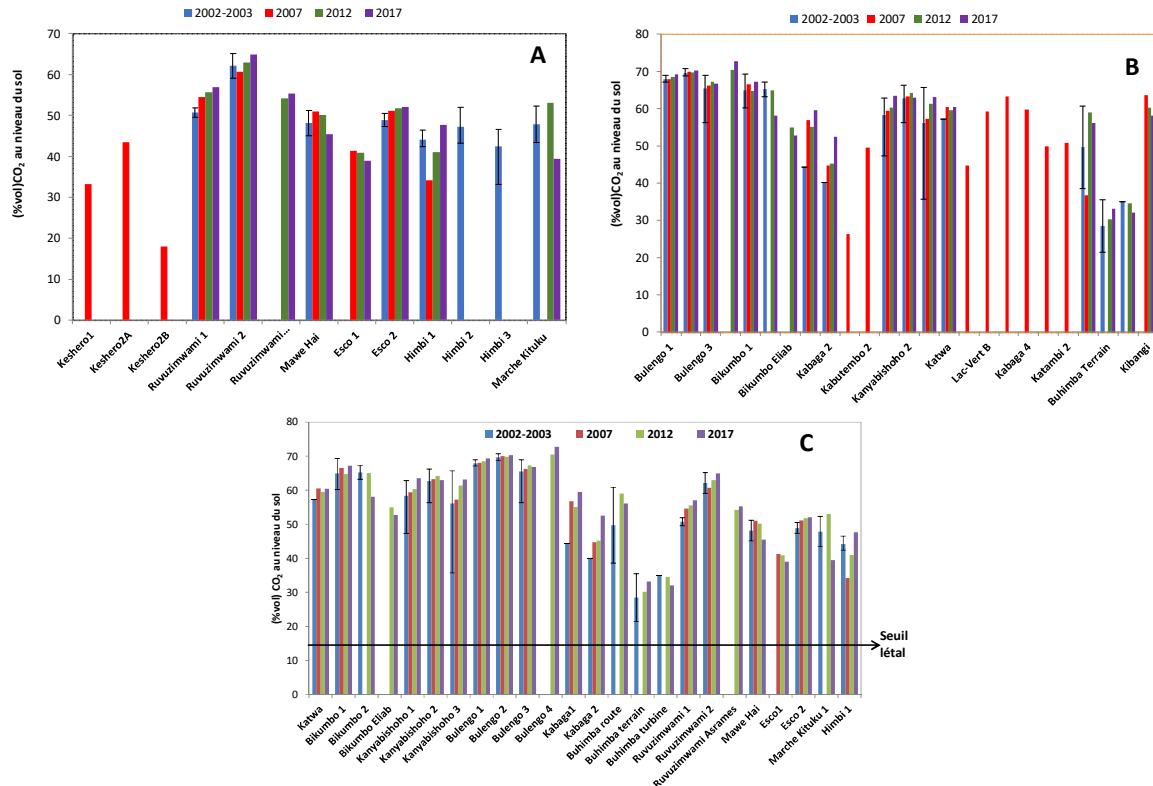


**Figure 7. Concentrations of CO<sub>2</sub> in the Mazuku shown in Figure 6, and showing that the values recently measured in 2017 are almost similar to those found in 2002 and 2003.**

Finally, Lake Kivu represents a significant hazard to Goma, but it also threatens the ~ 2.5 million people living on the other shores of the lake. Because Kabuno Bay contains a higher concentration of CO<sub>2</sub> than the other basins, and given the CO<sub>2</sub> rich-water is found at just ~11 m depth (Figure 5A), particular attention should be given to this part of the lake. Despite the fact that past lava inflows to Kabuno Bay did not cause a limnic eruption, the past response of the bay does not guarantee the same behavior during new lava inflows, particularly if they reach greater depths or are more voluminous. For now, the main basin and Kabuno Bay should be continuously monitored to identify, at an early stage, any increase in the gas concentrations to provide warning when the gas total pressure approaches saturation (Figure 5B). Because earthquakes and eruptions of Nyamulagira and Nyiragongo are also potentially capable of triggering an overturn of Lake Kivu, seismic and volcanic monitoring should not be separated from that of the lake. The observatory should include Lake Kivu monitoring into its routine activities, because monitoring the gases dissolved in Lake Kivu along with close surveys of

Nyiragongo and Nyamulagira volcanoes are the best means of prevention and mitigation of natural hazards in the region of Goma.

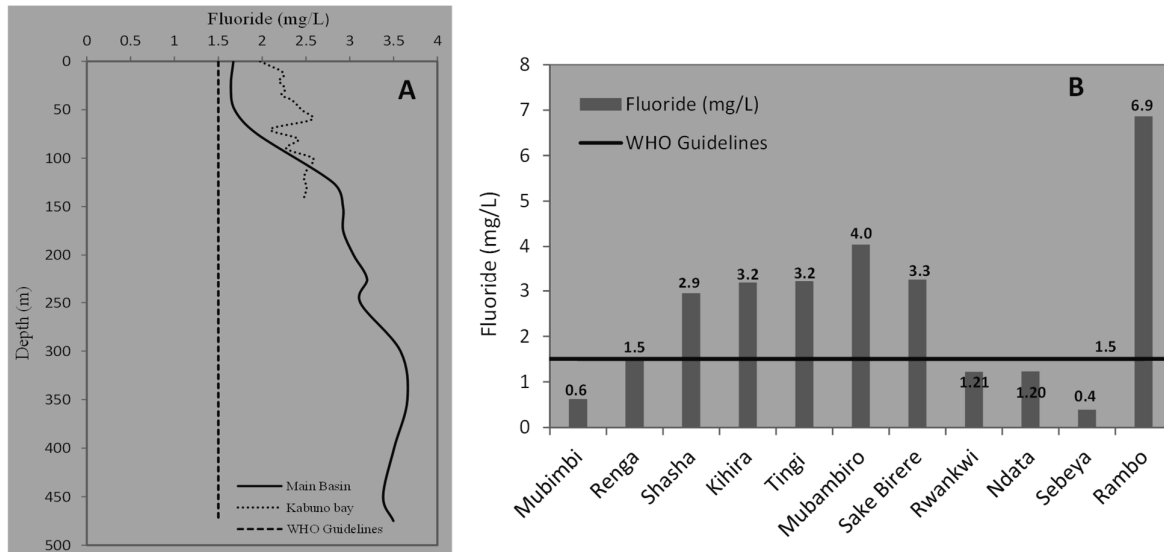


**Figure 8. (A) Vertical profiles of fluoride (mg/L) in the main basin of Lake Kivu and Kabuno Bay in February 2014. The vertical dotted line displays the WHO guideline recommendations (1.5 mg/L max) for drinking-water. (B) Fluoride concentration (mg/L) in the main rivers and springs in the area of Goma in February 2014. Sebeya and Rambo are located in Rwanda. The high volcanic activity of Nyiragongo and Nyamulagira volcanoes has led to high fluoride content in ground and surface water in the Virunga Volcanic Province.**



**Figure 9. Photos showing young and adult people affected with dental fluorosis disease in villages west of Goma where rivers and rainwaters contain fluoride greater than the WHO guidelines.**

### **5.1.3. Rain-plume interactions at Nyiragongo and Nyamulagira volcanoes and associated rainwater hazards, East Africa**

A rain-gauge network consisting of 13 stations was installed on the volcanic fields around Nyiragongo and Nyamulagira volcanoes, as well as in the surrounding villages and Goma city (DR Congo) (Figure 10) from December 2013 to October 2015. The rain gauges were then sampled on a monthly basis in order to assess the hazards related to the volcanic Nyiragongo and Nyamulagira plumes, through the evaluation of the influence of volcanic emissions, mainly the plume and ash on rain chemistry and rainwater quality, in a region where in many villages the population use only rainwater for all their daily activities (Figure 11). This is the first temporally distributed dataset of rain chemistry from this densely populated region, where the two Africa's most active volcanoes, 14 km apart, continuously eject gases and ash to the atmosphere (Figure 10) and where rainwater represents an important water resource. The results revealed that volcanic emissions are the primary source of the dissolved loads (Figure 12). Wind-blown dust dissolution is in fact occasionally the dominant source of major cations at cities and villages that are remote with respect to the volcano summits. A few sites located in the forested Virunga National Park are neither significantly impacted by volcanic emissions nor



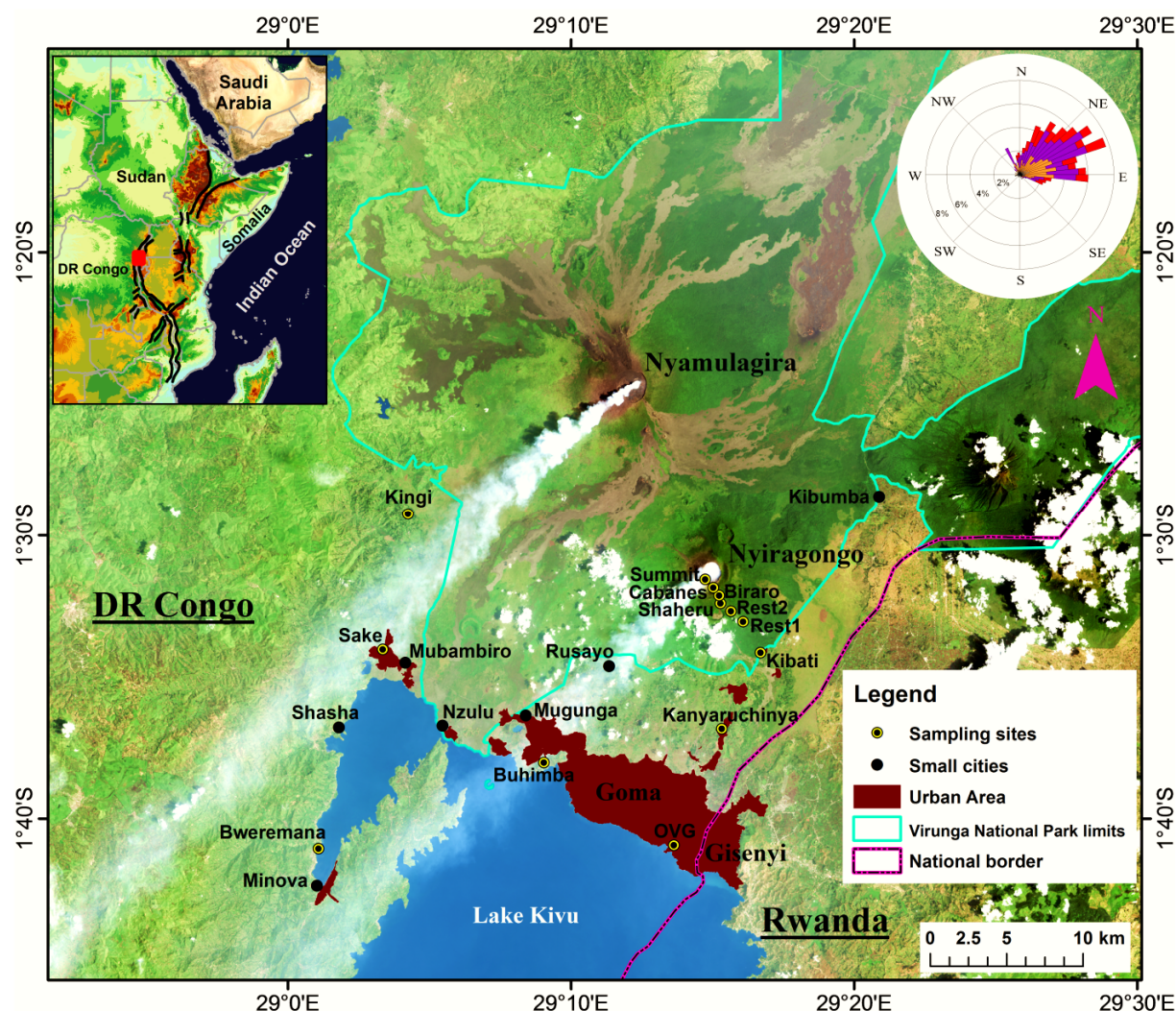


**Figure 10.** Locations of rain waters sampling sites around Nyiragongo and Nyamulagira volcanoes, which are situated within the western branch of the East African Rift System, as shown in the inset map. The sampling sites along the south flank of Mt Nyiragongo are in the following order, from farthest south to the crater at the volcano's summit: Kibati, Rest 1, Rest 2, Shaheru, Biraro, Cabanes and Summit. The base image, which was acquired on February 9, 2015 by NASA's Landsat 8 satellite, shows the permanent plumes from Nyiragongo and Nyamulagira volcanoes, which extend west-southwestward due to the dominant regional wind, as shown in the inset wind rose chart

wind-blown dust. The combined contribution of volcanic gases and the dissolution of volcanic ash and soil dust determined the pH of the rainwater. Thus, areas with limited volcanic impact showed higher pH values (up to 7.6), while those that experience major volcanic impact showed lower pH values (as low as 3.1) (Figure 12 A), as a consequence of the continuous input of acidic volcanic gases. The chemical composition of rain varies according to location and was driven by changes in wind direction. Nearly all the sites showed prominent temporal variations in

dissolved loads, which were essentially related to the variations in precipitation amount due to seasonal changes. The rain dissolved loads, the bulk atmospheric deposition fluxes (e.g., 0.5-24.6 t km<sup>-2</sup> yr<sup>-1</sup> for fluoride and 22.6- 176.6 t km<sup>-2</sup> yr<sup>-1</sup> for total dissolved substances, Table 5), and the spatial variations converged to show that localities to the west and southwest of Mt Nyiragongo are the most strongly impacted by volcanic emissions (Figure 13). These areas to the west and southwest, which experience higher rates of F deposition, also coincide with the locations of villages and small cities where endemic dental fluorosis occurs (e.g. in Figure 9). Such a relationship is explained by the use of F-rich water in all domestic activities, including as drinking water, in the region (e.g. Figure 11).



**Figure 11. Photos showing the techniques of rainwater harvest in villages located around Nyiragongo and Nyamulagira volcanoes, and where the rainwater is the unique water source which is thus used for all daily activities, including for drinking.**



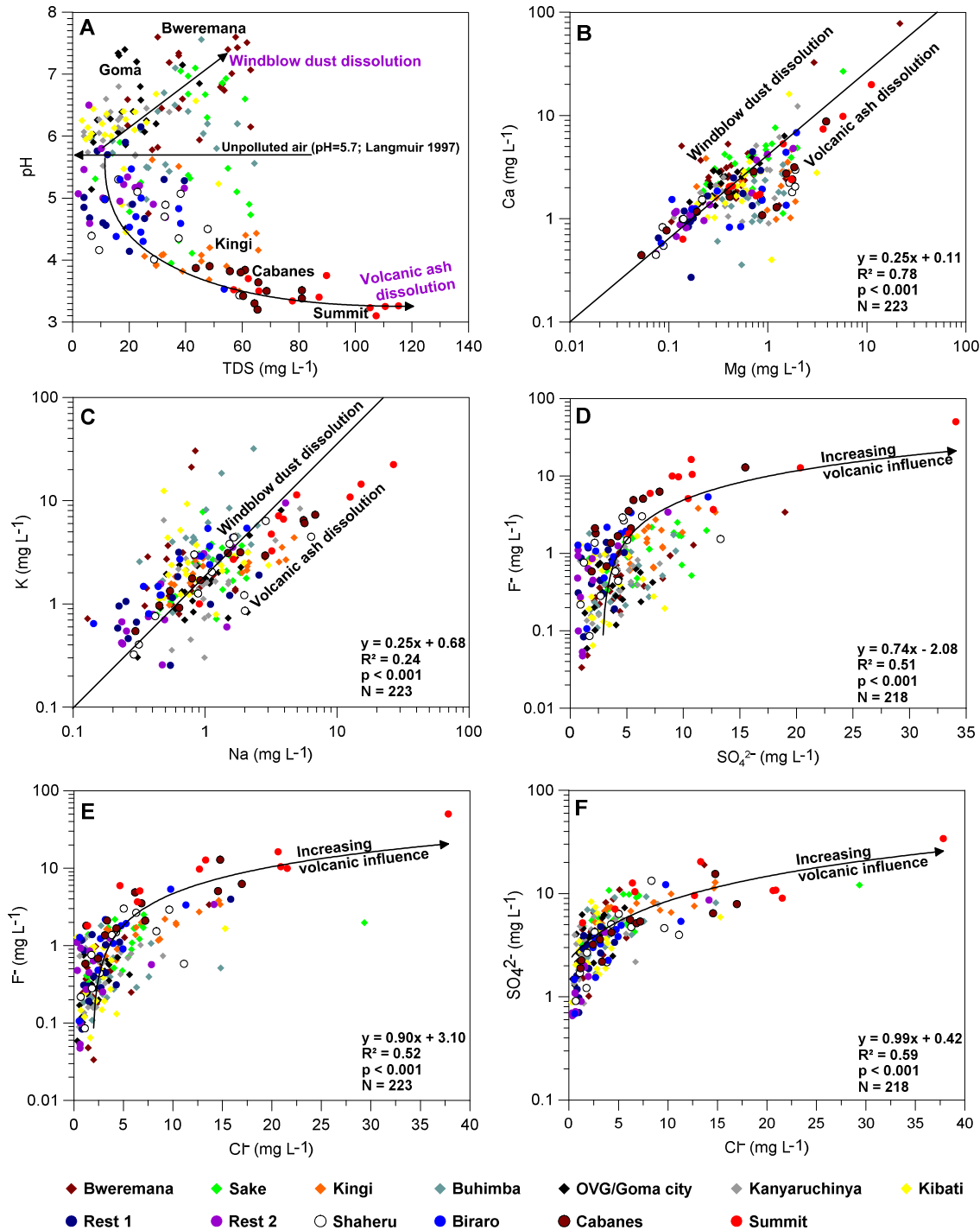


**Figure 12. Relationship between total dissolved substances and pH (A), Mg<sup>2+</sup> and Ca<sup>2+</sup> (B), Na<sup>+</sup> and K<sup>+</sup> (C), SO<sub>4</sub><sup>2-</sup> and F<sup>-</sup> (D), F<sup>-</sup> and Cl<sup>-</sup> (E), and Cl<sup>-</sup> and SO<sub>4</sub><sup>2-</sup> (F) in rainwater collected on a monthly basis in the Nyiragongo and Nyamulagira volcanic fields, in the northern basin of Lake Kivu, between December 2013 and December 2015.**

As main finding of this research we have:

- The permanent plumes of Nyiragongo and Nyamulagira have a great impact on the chemical composition of rain in the Virunga. In particular, rainwater from villages located to the west and southwest of the volcanoes showed higher dissolved loads, as consequence of regional winds that carry the volcanic emissions to these areas.
- Volcanic emissions are the primary sources of dissolved solutes. Their impact decreases with distance, and hence the contribution from soil dust (produced by wind and vehicles) gradually becomes important at remote sites, adding up to small amounts of solutes compared to those from volcanoes. Soil dust mainly impacts sites close to cities and large villages and areas undergoing significant deforestation and farming activities, which create conditions for dust production.
- In addition to the acid gases contained in the plume, the volcanoes also emit ash, of which the leaching and that of soil dust were pH-mediated. The leaching of both ash and soil contributed to enhance the rain solute contents.
- The annual seasonal changes, i.e., wet to dry and vice versa, yield precipitation variations which in turn govern the temporal variations in the dissolved loads in rain. The higher concentrations were accordingly recorded during the dry seasons, i.e., in July and August of each year.
- The dissolution of volcanic gases and ash leaching yielded rain enriched in chemicals. In particular, these processes led to F concentrations above the WHO recommendations for drinking water. The areas of more F-rich rainwater coincide with the location of villages and small cities where endemic dental fluorosis is observed. The dental fluorosis is thus a visible effect of the use of F-rich water in domestic activities, including as drinking water. However, even though rainwater is an important source of water in most villages and small cities around the active volcanoes of the Virunga, some localities that are remote with respect to these volcanoes contain springs, or are drained by surface rivers, or are located on the shores of Lake Kivu. In these localities, surface waters could be an additional contributing factor for the observed dental fluorosis.

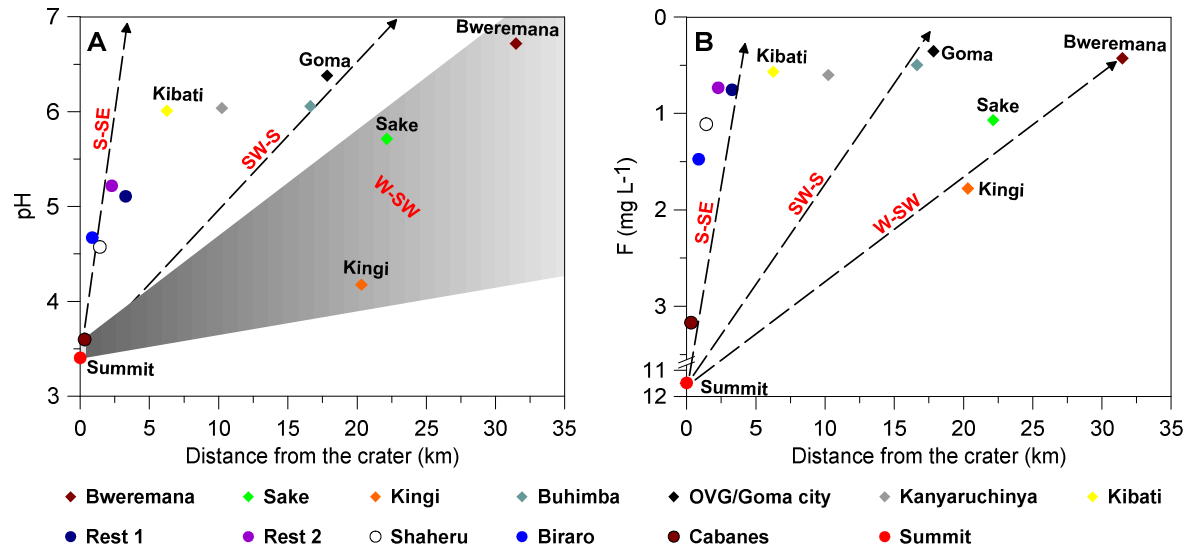


**Figure 13.** Spatial variations of mean pH (A) and fluorine (B) of rainwater based on the locations of the sites (both distance and orientation) with respect to Nyiragongo summit, which is set as the zero point. We used pH and fluorine for estimating the spatial variation with respect to volcanic emissions because these parameters are weakly affected by anthropogenic emissions. The dashed arrows indicate orientations towards the West-Southwest (W-SW), Southwest-South (SW-S) and South-Southeast (S-SE) from Nyiragongo summit. The black-gray zone shown in (A) represents the W-SW arc, the area that the volcanic plumes occupy most of time, based on the primary wind direction experienced by the region.

**Table 4.** Estimated annual bulk deposition fluxes of major anions and cations and Total Dissolved Substances in the Nyiragongo and Nyamulagira volcanic fields, as well as neighbouring areas in the north catchment of Lake Kivu. The annual fluxes were estimated based on the precipitation-weighted mean of solutes, and annual precipitation as collected in rain gauges. Data used for comparison at other volcanoes are from Bellomo et al. (2003), Liotta et al. (2006) and Aiuppa et al. (2001, 2006)

	Elevation (m a.s.l.)	Precipitation (mm/yr)	HCO <sub>3</sub> <sup>-</sup> (t/km <sup>2</sup> /yr)	F <sup>-</sup> (t/km <sup>2</sup> /yr)	Cl <sup>-</sup> (t/km <sup>2</sup> /yr)	SO <sub>4</sub> <sup>2-</sup> (t/km <sup>2</sup> /yr)	NO <sub>3</sub> <sup>-</sup> (t/km <sup>2</sup> /yr)	NH <sub>4</sub> <sup>+</sup> (t/km <sup>2</sup> /yr)	Na <sup>+</sup> (t/km <sup>2</sup> /yr)	K <sup>+</sup> (t/km <sup>2</sup> /yr)	Mg <sup>2+</sup> (t/km <sup>2</sup> /yr)	Ca <sup>2+</sup> (t/km <sup>2</sup> /yr)	Si (t/km <sup>2</sup> /yr)	TDS (t/km <sup>2</sup> /yr)
Bweremana	1470	1329.6	6.57	0.57	3.02	5.13	1.11	0.39	1.03	2.68	0.73	4.23	1.33	57.42
Sake	1514	1289.9	4.42	1.38	4.87	7.26	0.73	0.59	1.43	2.68	0.95	4.63	2.48	48.50
Kingi	1848	1597.5	0.46	2.84	11.92	11.64	1.13	2.36	3.33	3.74	1.66	3.55	4.21	66.56
Buhimba	1468	1414.8	5.82	0.70	4.86	6.00	0.04	0.10	1.38	6.31	1.07	2.21	1.45	46.12
OVG	1535	1254.2	5.32	0.45	2.36	4.40	0.15	0.29	1.12	1.68	0.40	2.63	2.20	22.61
Kanyaruchinya	1759	1671.9	6.70	1.00	3.75	6.24	0.26	0.23	1.82	3.44	0.95	3.48	2.83	22.63
Kibati	1994	1724.9	7.03	0.98	4.74	5.56	0.22	0.38	1.85	4.30	1.10	4.41	2.70	26.82
Rest 1	2254	2136.7	4.10	1.61	5.64	4.63	1.61	1.82	1.37	2.63	0.63	2.59	1.11	30.49
Rest 2	2535	2101.5	3.22	1.54	3.99	3.72	0.51	0.25	1.07	2.23	0.66	2.76	0.76	30.83
Shaheru	2761	2116.4	1.80	2.35	7.66	7.53	0.52	0.36	2.56	4.13	1.40	2.64	1.78	50.58
Biraro	2918	2332.2	2.09	3.44	7.93	7.54	0.38	0.63	1.47	4.79	1.40	3.91	1.47	54.22
Cabanes	3230	2124.1	0.00	6.73	12.04	9.75	0.50	1.30	4.16	5.45	2.06	4.32	4.69	129.43
Summit	3460	2095.2	0.00	24.05	29.64	24.05	3.19	2.94	15.75	17.71	5.27	10.40	6.91	176.56
Stromboli range <sup>ab</sup>	—	362-799	—	0.3-21.8	8.0-55.0	1.2-57.1	—	—	4.1-20.3	0.8-9.2	1.0-14.0	4.8-45.5	—	—
Etna <sup>ac,d</sup>	—	—	—	0.01-49.7	0.3-513.9	0.1-71.9	0.0-6.2	—	1.50-3.5	0.40-1.2	0.40-0.8	3.43-4.9	—	—
Virunga range	—	1254-2332	0.0-7.0	0.5-24.6	2.4-29.6	4.0-24.6	0.1-3.2	0.1-2.9	1.03-15.75	1.68-17.71	0.4-5.27	2.21-10.40	—	22.6-176.6



#### 5.1.4. Influence of moisture source dynamics and weather patterns on stable isotopes ratios of precipitation in Central-Eastern Africa

In the present research we report the first  $\delta^{18}\text{O}$  and  $\delta^2\text{H}$  data of Virunga rainfall in the Eastern Democratic Republic of the Congo, situated on the limit between Central and Eastern Africa. The dataset is from 13 rain gauges deployed at Mount Nyiragongo and its surroundings (Figure 14) sampled monthly between December 2013 and October 2015. The  $\delta^{18}\text{O}$  and  $\delta^2\text{H}$  vary from

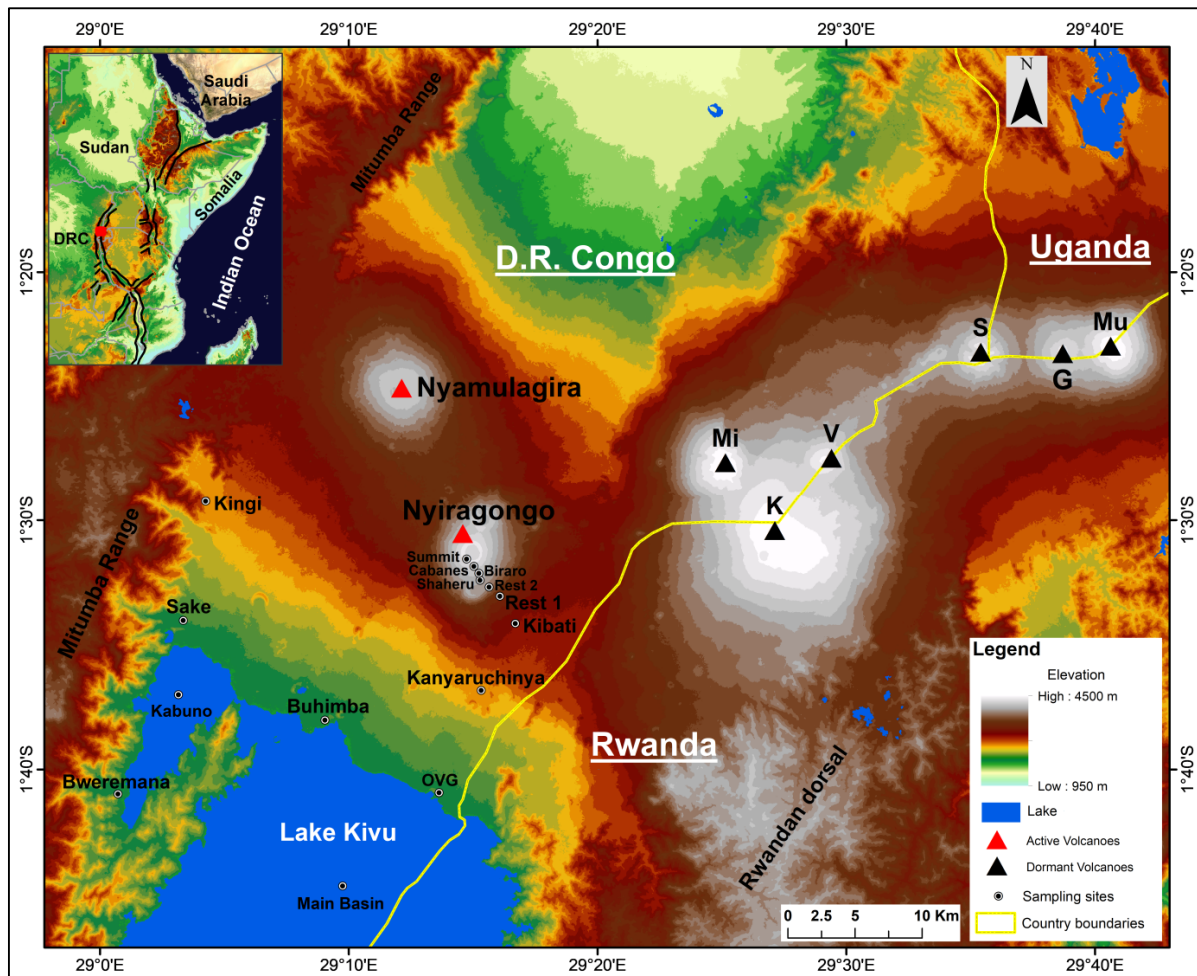


**Figure 14.** Topographic map of the study area situated within the western branch of the East African Rift System (shown in the inset map). The sampling sites along the southern flank of Mt Nyiragongo are in the following order, from farthest south to the volcano's summit: Kibati (1994 m above sea level, m a.s.l.), Rest 1 (2254 m a.s.l.), Rest 2 (2535 m a.s.l.), Shaheru (2761 m a.s.l.), Biraro (2918 m a.s.l.), Cabanes (3230 m a.s.l.) and Summit (3460 m a.s.l.). The Virunga chain of mountains are oriented EW and perpendicular to the axis of the Western Branch, and include Mt Nyamulagira (3058 m a.s.l.), Mt Nyiragongo (3470 m a.s.l.), Mt Mikeno (Mi, 4437 m a.s.l.), Mt Karisimbi (K, 4508 m a.s.l.), Mt Visoke (V, 3911 m a.s.l.), Mt Sabinyo (S, 3647 m a.s.l.), Mt Gahinga (G, 3474 m a.s.l.), and Mt Muhabura (Mu, 4127 m a.s.l.).

- 6.44 to 6.16‰, and -32.53 to 58.89‰ respectively, and allowed us to define a LMWL of  $\delta^2\text{H}=7.60\delta^{18}\text{O} + 16.18$ . Three main wind directions, i.e. NE, E and SE, were identified in the upper atmosphere (Figure 15B) corresponding to three major moisture source regions (Figure 16). On the contrary, lower atmospheric winds are weaker in nature and originate mainly from the S and SW, creating a topographically-driven, more local moisture regime (Figure 15A). The latter is due to the accumulation in the floor of the rift of water vapor from Lake Kivu forming a layer of isotopically enriched vapor that mediates the isotope enrichment of the falling raindrops. A strong seasonality is observed in both  $\delta^{18}\text{O}$  and  $\delta^2\text{H}$  data (Figure 18), and is primarily driven by combined seasonal and spatial variation in the moisture sources. The  $\delta^{18}\text{O}$  and  $\delta^2\text{H}$  seasonality is thus correlated to weather patterns, as the latter control the wet to dry season shifting, and vice versa (Figure 19). The key characteristic of seasonality is the variation of monthly precipitation amounts, since the mean monthly air temperature is nearly constant on an annual scale. Two regionally relevant hydrological processes contribute to the isotopic signature: namely moisture uptake from the isotopically enriched surface waters of East African lakes and from the depleted soil-water and plants. Consequently, the proportion of water vapor from each of these reservoirs in the atmosphere drives the enrichment or depletion of  $\delta^2\text{H}$  and  $\delta^{18}\text{O}$  in the precipitation. Thus, during wet periods the vapor from soil-plants evapotranspiration dominates yielding isotopically depleted precipitation, contrary to dry periods when vapor from lakes surface evaporation dominates, yielding isotopically enriched precipitation. At the global scale, our dataset reduces gaps in this region that has been poorly studied for  $\delta^{18}\text{O}$  and  $\delta^2\text{H}$  in precipitation. At the regional scale, the improved understanding of the ways land cover, moisture source seasonal and spatial dynamics, and atmospheric patterns impact precipitation spatial and temporal variabilities in Central-East African contribute to the ongoing research on mitigating the impacts of ongoing climate change in Sub-Saharan Africa. The reduction of gaps and uncertainties in  $\delta^2\text{H}$  and  $\delta^{18}\text{O}$  of precipitation, and the understanding of their interrelation with weather patterns are essential for a better past, present and future environmental and climatic modelling at both local and regional scales.

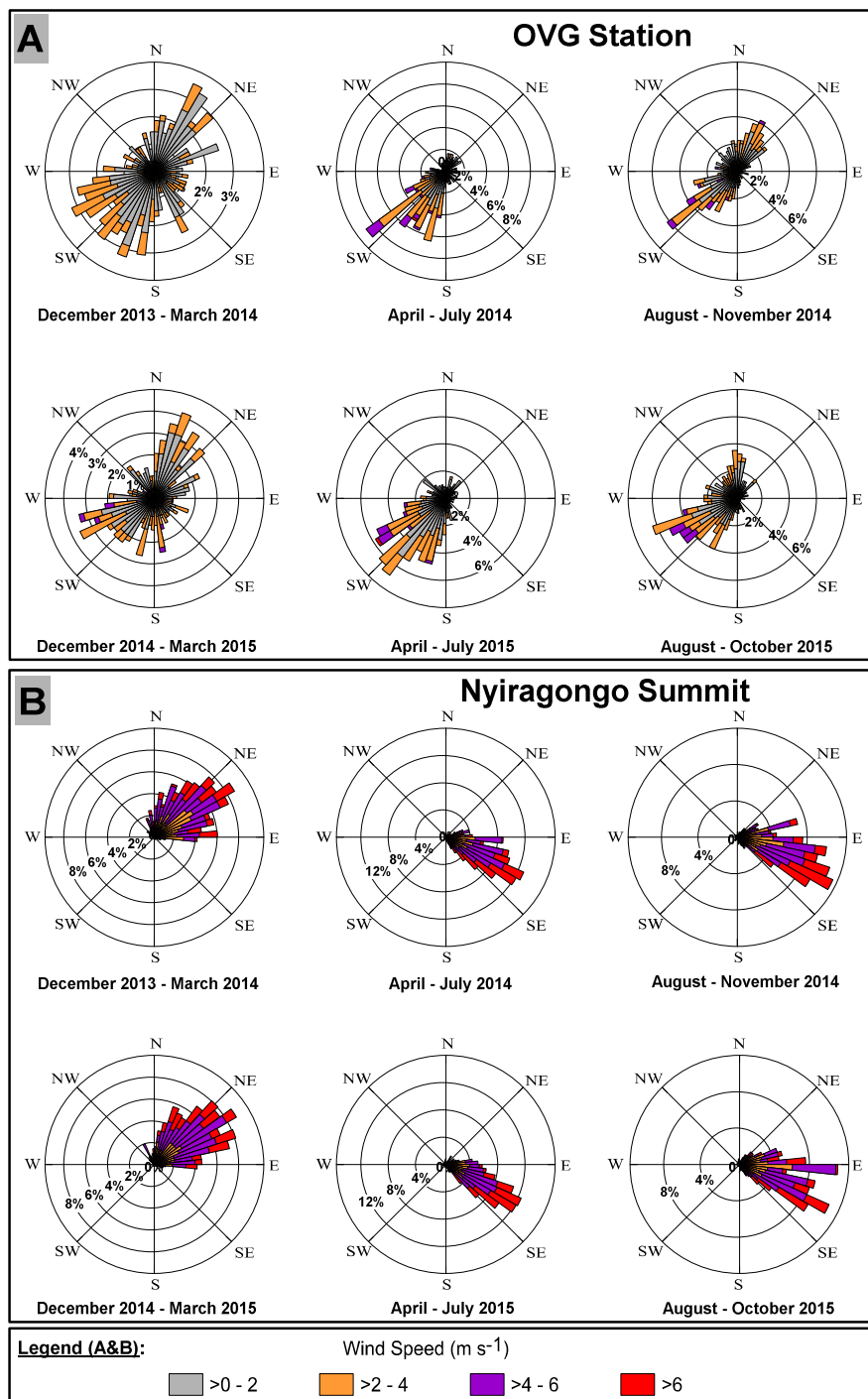


**Figure 15. Rose charts of annual main wind directions and speeds at OVG station (A) and the summit of Mt Nyiragongo (B) (at 700 mbar) between December 2013 and October 2015. The grouped data were daily wind direction and speed collected on 6 hours intervals by the ERA-Interim model of the European Centre for Medium-Range Weather Forecast (ECMWF).**

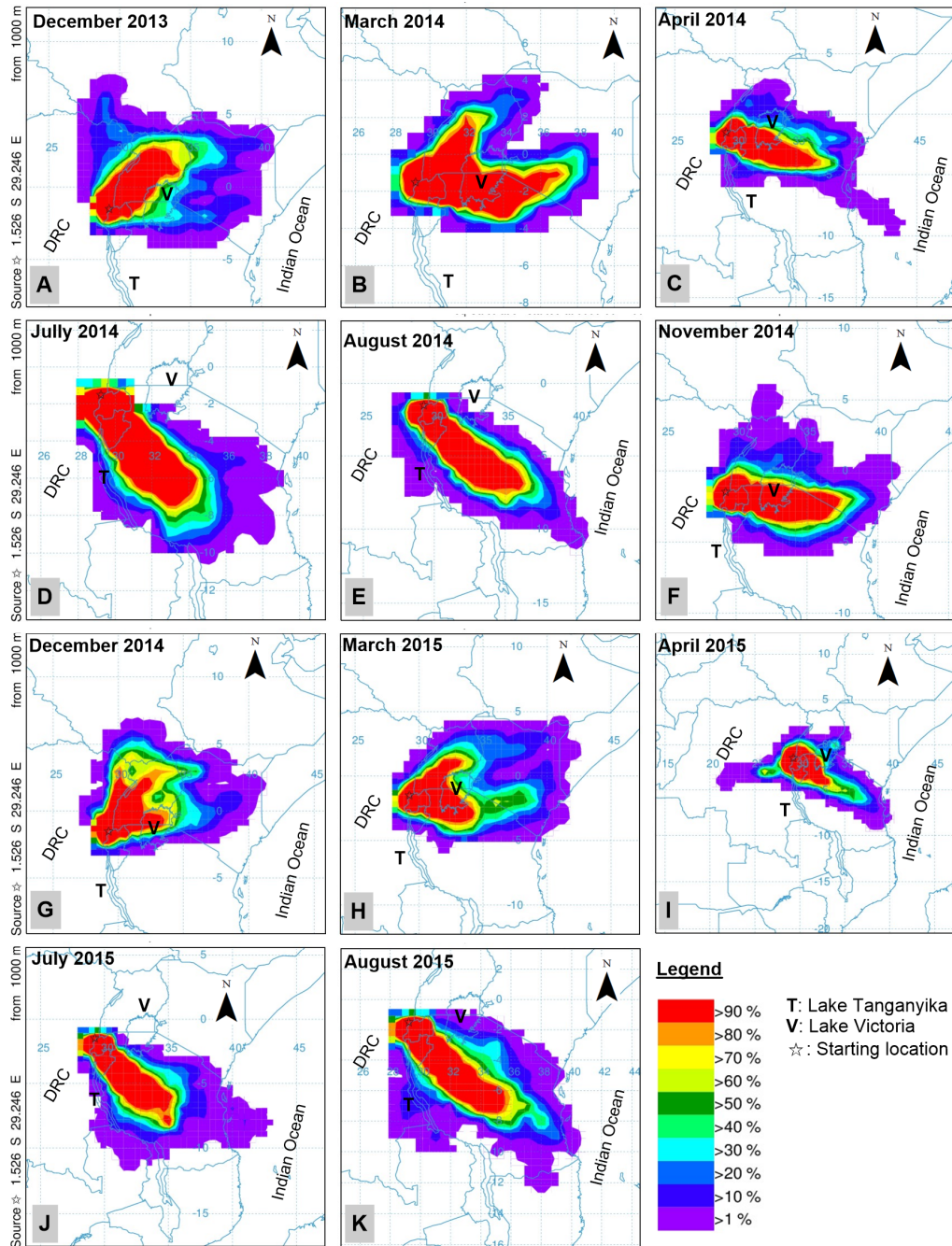


**Figure 16.** Backward 48 hours trajectory frequency plots from a starting location at the summit of Mount Nyiragongo (1.52S, 29.25E) indicated by the star in the charts. For each chart the contours represent, in percentage, the likely moisture source area that yielded the formation of precipitation at the starting location. On an annual scale time, the moisture source region changes as a result of the observed variation in wind direction.



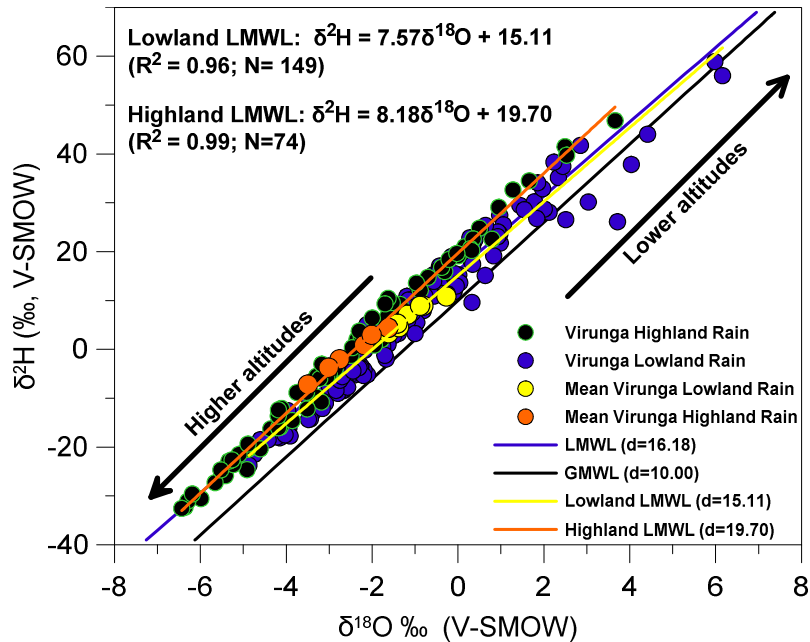


**Figure 17.** Relationship between  $\delta^2\text{H}$  and  $\delta^{18}\text{O}$  from monthly, mean lowland and highland rainwater at Mt Nyiragongo and the surrounding in the Eastern Democratic of the Congo, between December 2013 and October 2015. The lowland and highland refer to areas situated below and above 2000 m a.s.l., respectively; the whole sampling sites being between 1460 and 3470 m a.s.l of altitude.

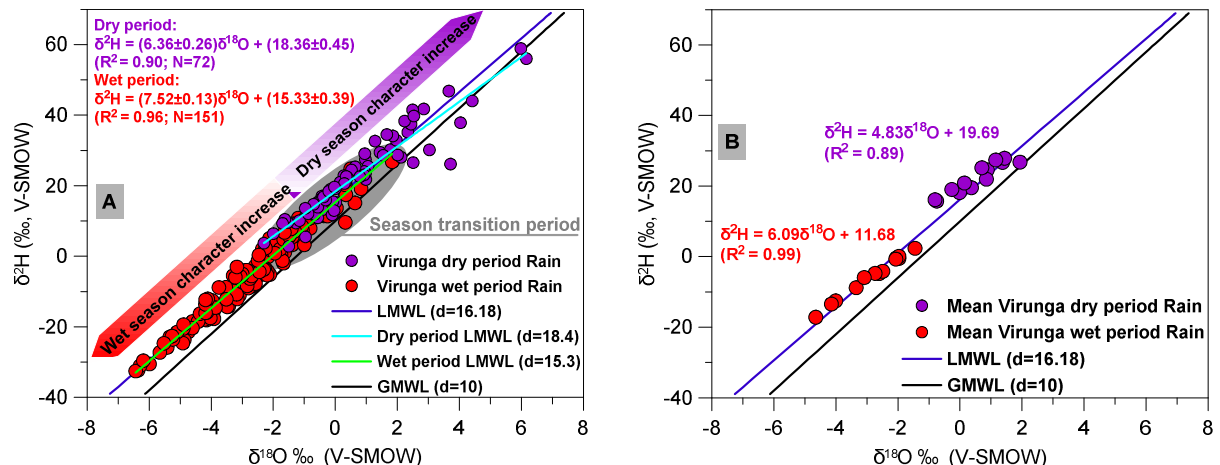


**Figure 18.** Plots of monthly  $\delta^2\text{H}$  versus  $\delta^{18}\text{O}$  (A) and mean  $\delta^2\text{H}$  versus  $\delta^{18}\text{O}$  (B) in precipitations at Mount Nyiragongo and the surrounding, in the Eastern Democratic of the Congo, between December 2013 and October 2015. The red dots represent  $\delta^2\text{H}$  and  $\delta^{18}\text{O}$  from rainwater samples collected during the wet periods (mainly the rain season) while the violet dots represent values from dry periods (mainly dry the season).

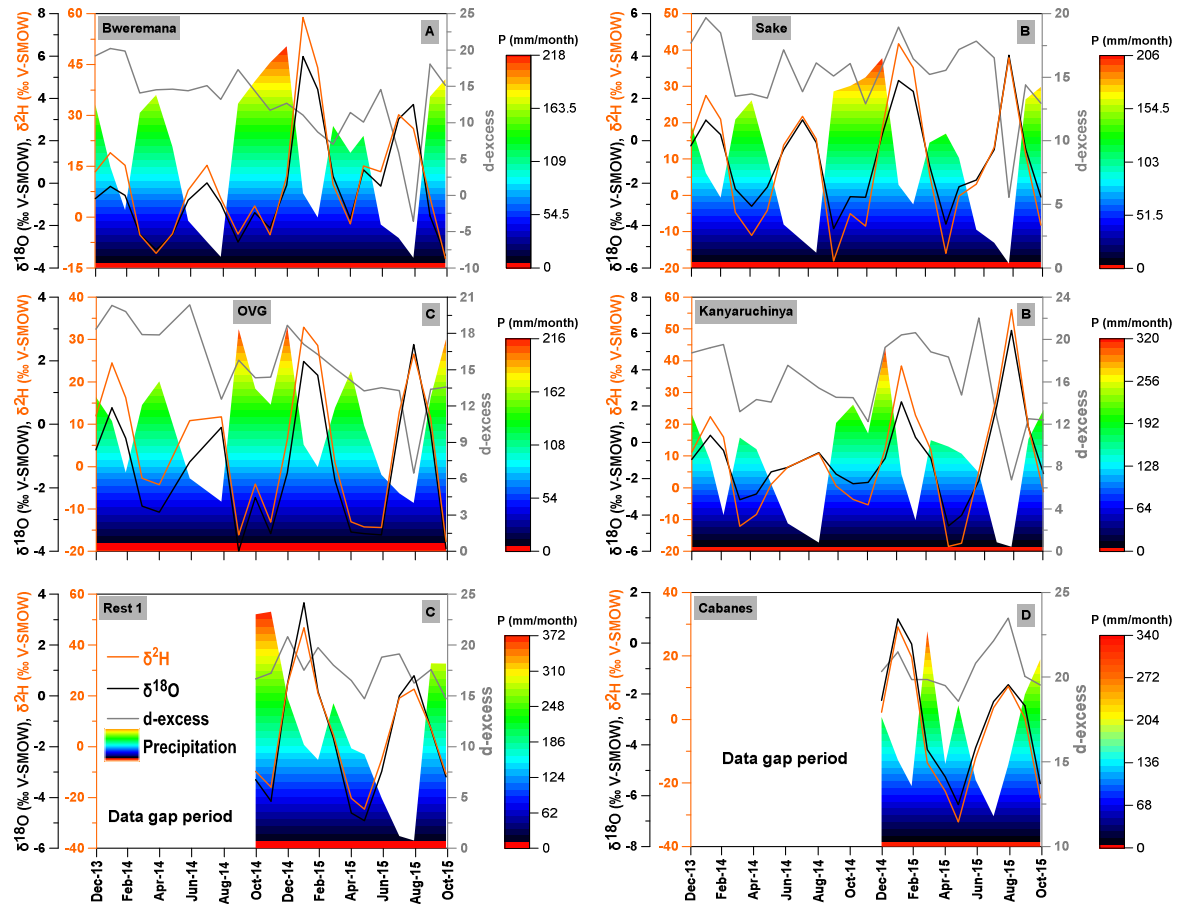


**Figure 19. Temporal evolution of monthly  $\delta^2\text{H}$ ,  $\delta^{18}\text{O}$  and d-excess in precipitation at Mount Nyiragongo and its surroundings, in the Eastern Democratic of the Congo, between December 2013 and October 2015. The monthly precipitation values are shown in each plot to highlight the changes in monthly  $\delta^2\text{H}$ ,  $\delta^{18}\text{O}$  and d-excess as a response to monthly precipitation change.**

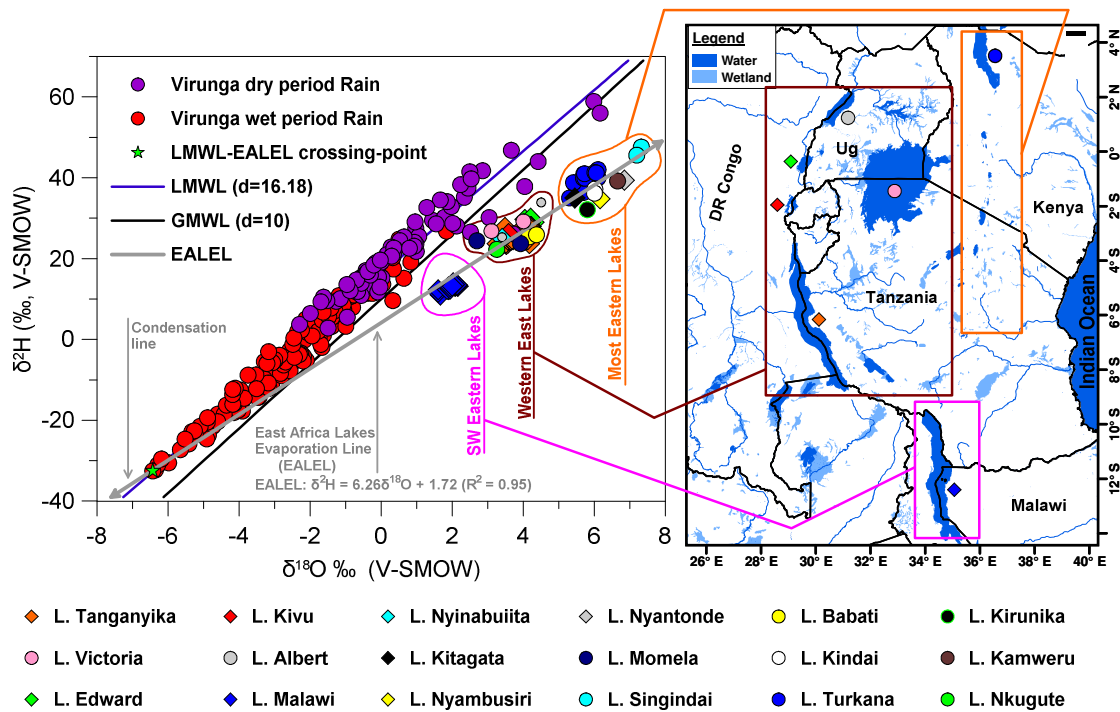


**Figure 20.** Plot of oxygen and hydrogen isotope composition for Virunga precipitation and East African lakes surface waters. The lakes in the East African lakes group are located to the East of the longitude E35°, the western group are to its west, and the southwestern group is similarly found to the west with a further southward trend. Data for Virunga precipitation are from this study, lakes data are from Craig 1975, Gonfiantini et al., 1979; Cerling et al., 1988; Odada et al., 2001; Bahati et al., 2005; Cockerton et al., 2013 and Jasechko et al., 2013.

#### **5.1.5. Volcanic risk assesment in the Democratic Republic of the Congo**

The Virunga Volcanoes Supersite requested the present mapping from the Copernicus Emergency Management Service of which purpose was to generate comprehensive knowledge through performing pre-disaster situation analysis, concerning a potential eruption of the Nyiragongo volcano located near the city of Goma. Thus, the specific activation focused on pre-disaster situation analysis; more specifically it addresses risk analyses with a focus on volcanic hazard, in term of assessment of the impact of a potential Nyiragongo volcano eruption to the surrounding urban agglomerations and infrastructures. Furthermore, it aimed at producing a very highly accurate Digital Elevation Model (DEM) to simulate lava flow pathways for future eruptions management, and an assessment of pertinent evacuation pathways/means. Towards supporting informed decision making of the involved stakeholders with reference to disaster preparedness and disaster management, an evacuation plan was also carried out. Moreover, Land Use/Cover and Reference Information were generated to assess the assets that might be most affected by a lava eruption event. Towards adequate disaster evaluation, a very high-resolution Digital Elevation Model with 5 m grid spacing and vertical accuracy of 3m was also created.

##### **➤ List of generated products**

#### **1. REFERENCE MAPPING; Topographic elements, Settlements, transport network, POIs, etc.**

OSM Data Integration and Data Capture from the Very High-Resolution satellite images (2017); Digitization of buildings footprints (large structures/ POIs), road network digitization and harmonization, buildings information enrichment (use: education, governmental facilities, hospitals, etc.) through visual inspection of Geo-portals, etc. Goma city road network, Goma urban area limit - populated zones, Hydrographic Network, Education (schools), Health (hospitals) POIs and vegetation (see Figure 21).

#### **2. LAND USE AND COVER MAPPING**

OSM Data Integration and Data Capture from the VHR satellite images (2017); Delineation and assignment of LULC categories on the basis of the optical data at 1:10.000 scale (see Figure 22).

#### **3. Digital Elevation Model**

Digital Elevation Model, through processing monostatic Tandem-X couples and a Pleiades panchromatic stereo-pair. The products obtained from SAR and optical data processing were then fused, using weighting parameters, calculated during the generation process. The result was a detailed DEM with a 5 meters grid spacing and a vertical accuracy of 3 meters (refer to online version at <https://emergency.copernicus.eu/mapping/list-of-components/EMSN047>).



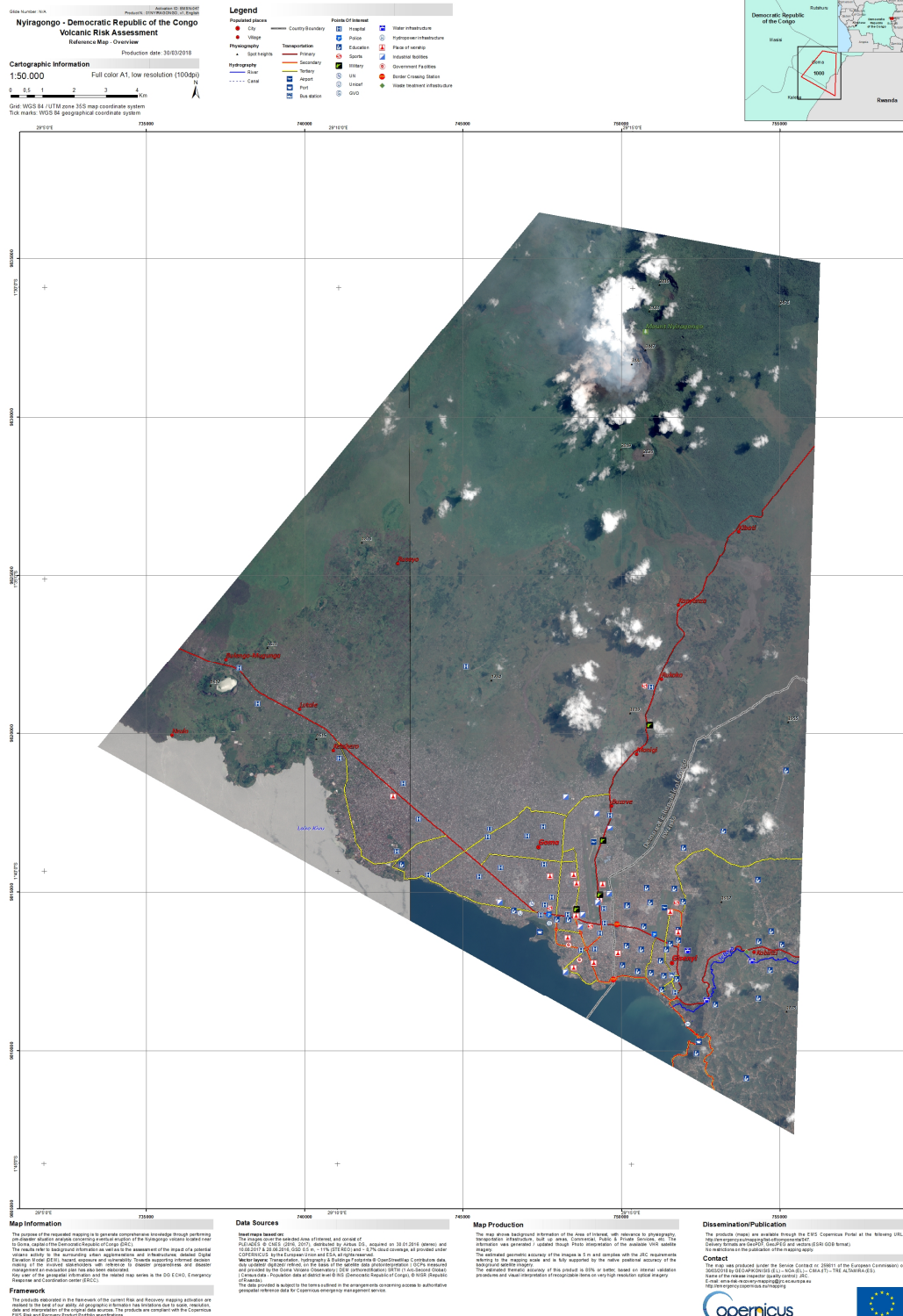


**Figure 21. REFERENCE MAPPING; Topographic elements, Settlements, transport network, POIs, etc. map for Nyiragongo Volcano and the city of Goma developed in 2018 by the COPERNICUS - EMERGENCY MANAGEMENT SERVICE RISK & RECOVERY MAPPING, EMSN 047 Volcanic risk in Democratic Republic of the Congo"**

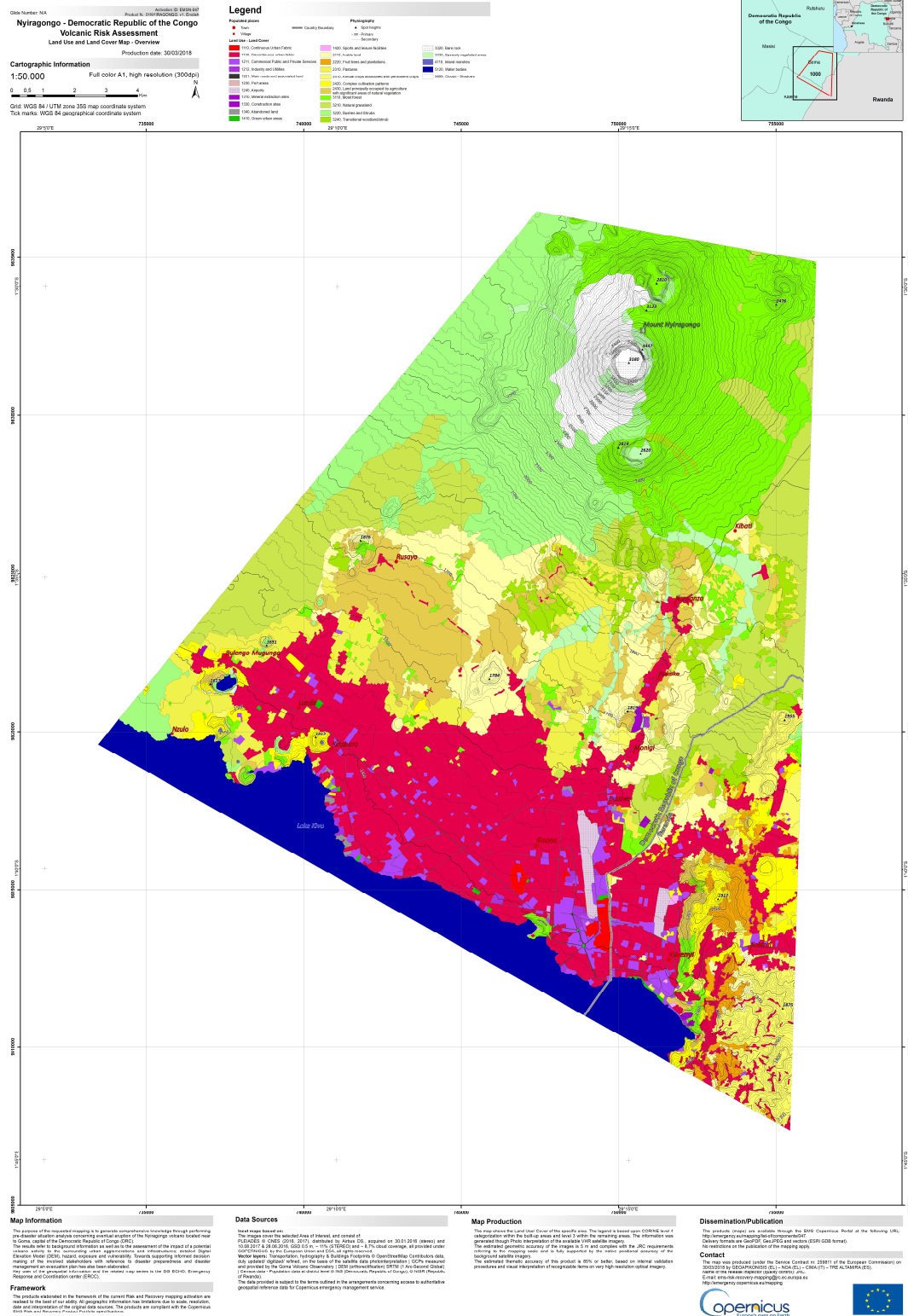


**Figure 22. Map of land use and cover for Nyiragongo Volcano and the city of Goma developed in 2018 by the COPERNICUS - EMERGENCY MANAGEMENT SERVICE RISK & RECOVERY MAPPING, EMSN 047 Volcanic risk in Democratic Republic of the Congo"**

#### **4. Lava Flow Hazard/ Exposure of assets and population**

The **Lava Flow Hazard** assessment was determined by performing data analysis based on modified and extended implementations of (i) the QVAST tool for the estimation of volcanic susceptibility and (ii) the Q-LavHa tool for the estimation of the lava flow paths and their convergence, by exploiting probabilistic and deterministic simulation models for evaluating channeled lava flow inundation probabilities from regularly distributed eruptive vents. The applied processing involved: (i) the study of the historical volcanic activity of the area (analysis of historic eruption fissure and vent locations), (ii) Calculation of a volcanic eruption susceptibility map, obtained through a non-homogeneous Poisson process (NHPP) on the basis of Probability Density Function (PDF) Maps and definition of the possible lava eruption areas and (iii) Per pixel (DEM) estimation of lava inundation probability (Q-LavHa tool models). Data on exposed assets are provided in relative tables per Hazard Level. An evacuation Plan was also developed through accounting for topography and the available road network (see Figure 23).

#### **5. Road Network Vulnerability to Disruption**

Estimation of Vulnerability of disruption is based upon: the Road capacity, as inferred by the respective taxonomy (highway, primary, secondary, etc.), proximity to populated places, and availability of alternative routes. The vulnerability to disruption is estimated for each road segment (five discrete classes) (see Figure 24).



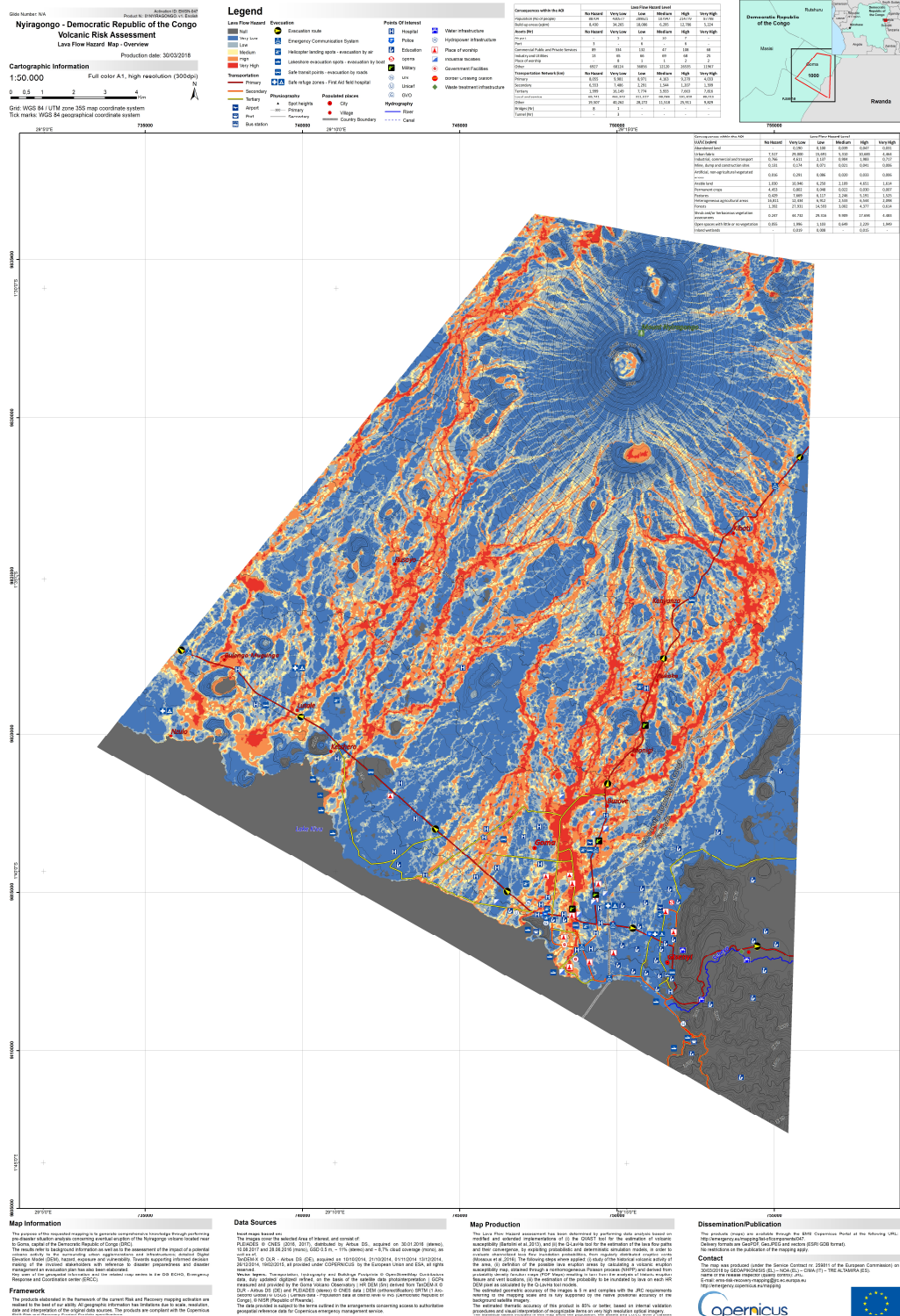


**Figure 23. Lava Flow Hazard/ Exposure of assets and population map for Nyiragongo Volcano and the city of Goma developed in 2018 by the COPERNICUS - EMERGENCY MANAGEMENT SERVICE RISK & RECOVERY MAPPING, EMSN 047 Volcanic risk in Democratic Republic of the Congo**

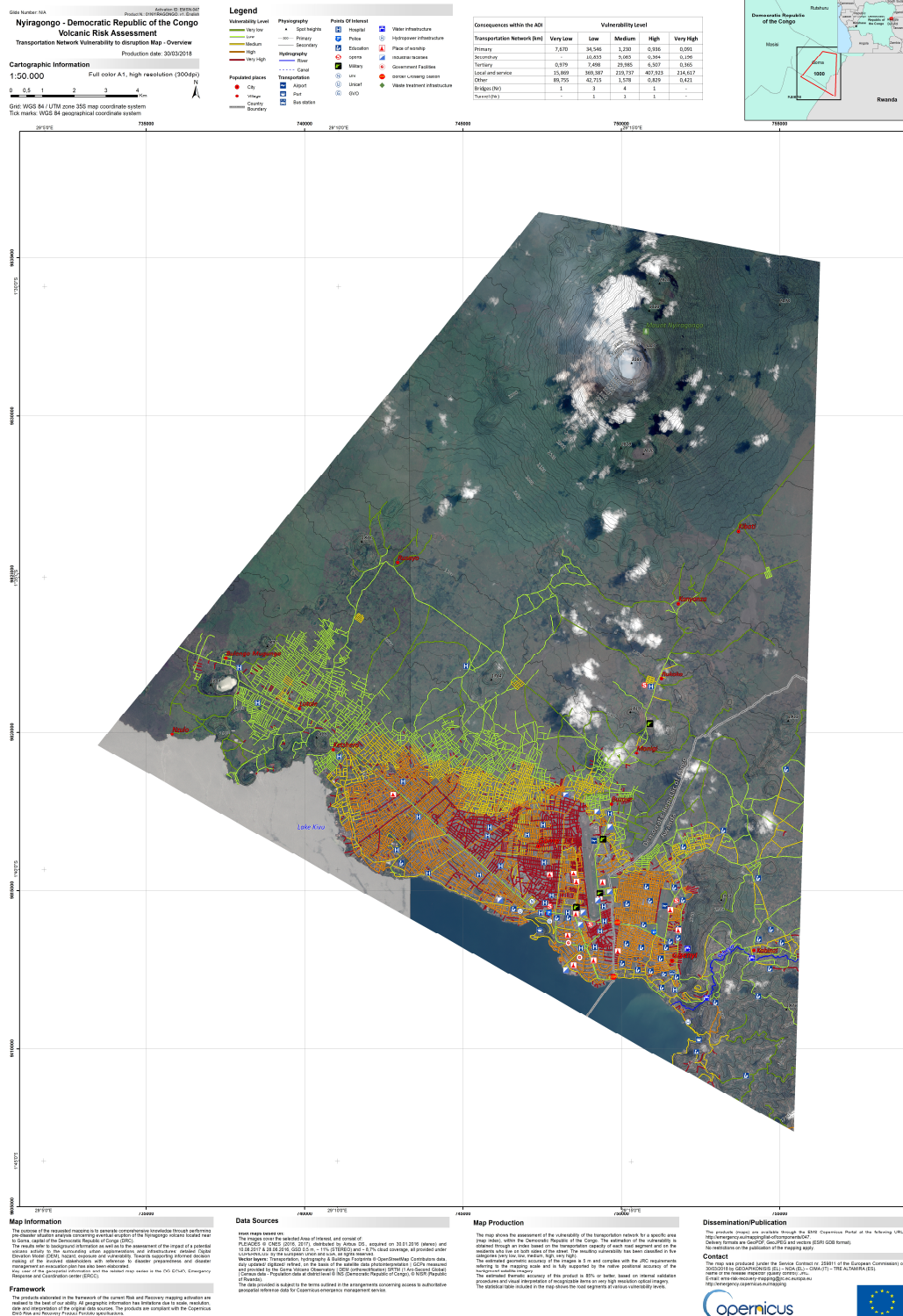


**Figure 24. Map of Road Network Vulnerability to lava from Nyiragongo Volcano, in the city of Goma developed in 2018 by the COPERNICUS - EMERGENCY MANAGEMENT SERVICE RISK & RECOVERY MAPPING, EMSN 047 Volcanic risk in Democratic Republic of the Congo**



### 5.1.6. Monitoring CO<sub>2</sub>, SO<sub>2</sub> and H<sub>2</sub>S concentrations in Nyiragongo volcanic plume using MultiGas techniques

Two members of the Goma Volcano Observatory composed of Researcher Geochemist and a Technician attended a Multi-Gas training seminar organized in Vancouver-Washington at the Cascades Volcano Observatory by the Volcano Disaster Assistance program, from 15 June to 13 July 2019. After the training a Portable Multi-Gas station was donated to the Goma Volcano Observatory to support the monitoring of CO<sub>2</sub>, SO<sub>2</sub> and H<sub>2</sub>S in the volcanic plume of Nyiragongo volcanic plume.

Since September 2019 the portable MultiGas is being regularly deployed at the summit of Nyiragongo. The preliminary results show that the bulk gas composition is 39.31%, 59.93 % and 0.76 % for H<sub>2</sub>O, CO<sub>2</sub> and SO<sub>2</sub>, respectively with minor amount of H<sub>2</sub>S. We have been able to identify two main compositions based on CO<sub>2</sub>/SO<sub>2</sub> (Figure 25), with one end-member showing CO<sub>2</sub>/SO<sub>2</sub> of about 50-60 and another with a much higher ratio with value up to 300 (Figure 26).

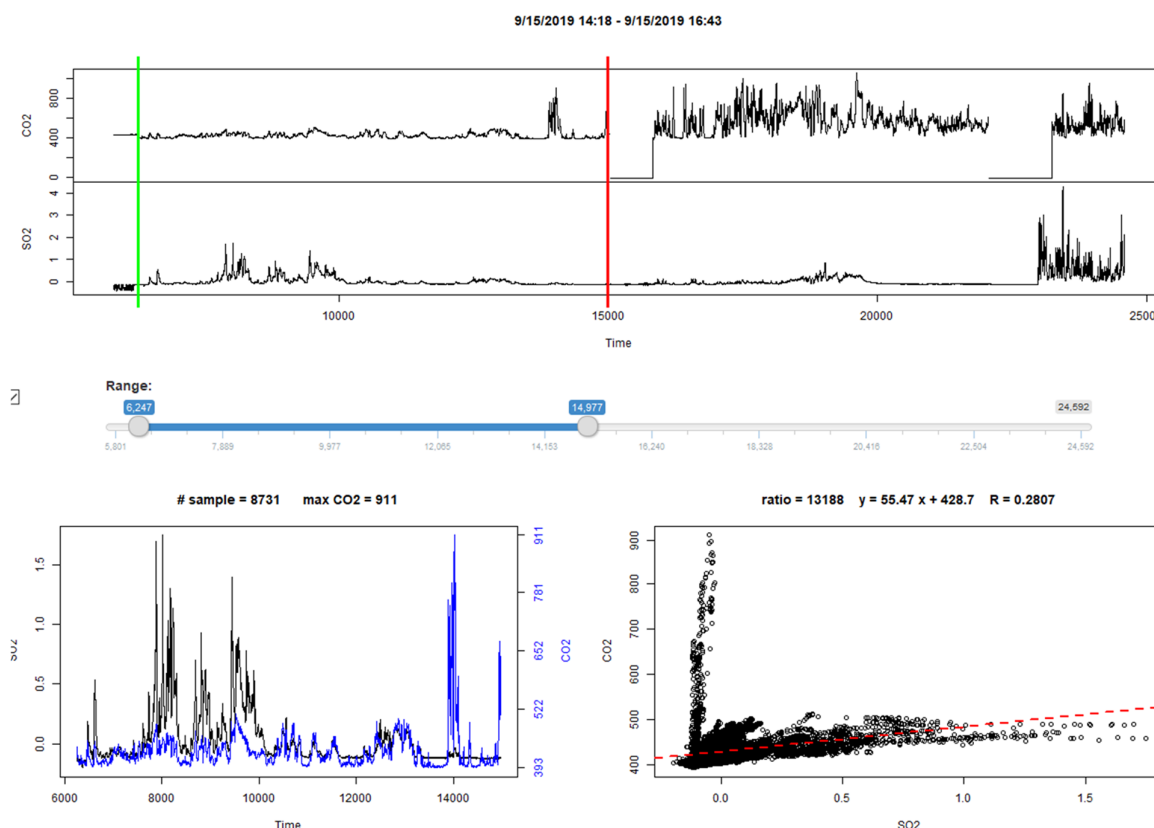


**Figure 25. Upper chart: SO<sub>2</sub> and CO<sub>2</sub> data as measured at the crater rim of Nyiragongo volcano using a portable MultiGas. Lower chart: CO<sub>2</sub> versus SO<sub>2</sub> from data selected in the upper chart, i.e. the data found between the vertical green and red lines.**

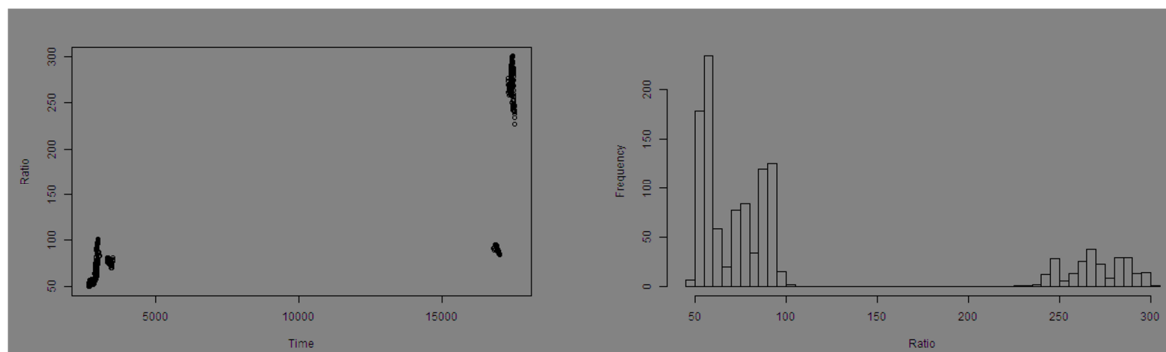


**Figure 26. CO<sub>2</sub>/SO<sub>2</sub> ratios in Nyiragongo volcanic plume obtained using a portable MultiGas instrument, campaign of September 2019.**

## 5.2. Satellite Data

### 5.2.1. SAR Data

The Virunga region has been observed by a large number of SAR data acquired by different space agencies (e.g. ASI, ESA), with a twofold aim: to deeply investigate and monitor over space and time the Nyiragongo and Nyamulagira active volcanoes, thus estimating how much magma is stored beneath the two volcanic edifices and understanding the rift-zone volcanism, and also to identify and map the location of normal and non-normal faults in correspondence to the northern and southern Lake Kivu Basin, whose activities are linked to that of the rift and along which the major impacts of past earthquake events have been located so far.

Within the first two years of the Supersite project, we concentrated on the first issue (the rift-zone volcanism). Here we present the results, achieved by the CNR-IREA research team, relevant to the surface deformation analysis, performed over the Virunga region, through the advanced Differential Synthetic Aperture Radar Interferometry (DInSAR) technique referred to as SBAS (Small BAseline Subset) along the 2011 - 2019 time interval. In particular, we used 476 SAR data collected by the X-band COSMO-SkyMed (CSK) constellation of the Italian Space Agency (ASI), acquired along descending orbits during the April 2011 – February 2019 time interval, and 84 SAR data of the C-band Sentinel-1 (S-1) constellation of the European Copernicus Programme, acquired along descending orbits along the June 2016 - October 2019 time period. Starting from the available SAR acquisitions, we identified two sets of interferometric data pairs, by imposing constraints on the maximum spatial and temporal baseline values (e.g. 500 m and 400 days for the CSK interferometric dataset). Then, 1479 CSK and 221 S-1 DInSAR interferograms were generated, using the 1-arcsec Shuttle Radar Topography Mission (SRTM) DEM of the study area to remove the topographic phase component. A sketch of the main characteristics of the exploited CSK and S-1 SAR datasets is reported in Table 5 and 6, respectively.

We applied the advanced DInSAR technique referred to as SBAS (Small BAseline Subset) to the

selected differential interferograms. The SBAS approach, developed by the researchers of IREA-CNR in 2001, is based on the generation of differential interferograms, obtained by computing the phase difference between two SAR images collected over the same area at different epochs (temporal baseline) and with slight different orbital positions (spatial baseline). A proper combination of a large number of differential interferograms (by means of the Singular Value Decomposition method) allows generating mean deformation velocity maps and corresponding time series. The use of small spatial and temporal baseline of the DInSAR interferograms permits mitigating the decorrelation phenomena that affect the interferometric pairs, and thus drastically increases the spatial density of the retrieved DInSAR measurements (coherent pixels), especially in semi-urbanized and rural areas. Moreover, within the SBAS approach a filtering operation is performed to detect and remove atmospheric artifacts from the displacement time-series. Accordingly, for each coherent pixel of the investigated scene, the SBAS technique permits to follow the temporal evolution of the retrieved radar Line of Sight (LOS)-projected displacements, which are referred to a spatial point of the scene that is considered stable, and to a temporal reference that usually corresponds to the first available acquisition.

In Figure 27 we show the LOS mean deformation velocity map of the CSK data processing, superimposed on an optical image of the investigated area, relevant to the coherent pixels only. According to the color bar depicted in Figure 27, green color represents areas that are stable in terms of surface displacements, whereas the red and blue colors stand for negative and positive deformation velocity values, which correspond to an increase and decrease of the LOS sensor-to-target distance, respectively. Pixels where the deformation value is not reliable (low coherent pixels) are excluded from the map.

The analyzed area extends for about 40 x 40 km<sup>2</sup> and mainly covers the Nyamulagira active volcano, where a significant deformation signal of more than 3 cm/year has been detected in correspondence to a large part of the volcanic edifice, very likely due to the magma movements. Some deformation phenomena of more than 2 cm/year have also been detected in the southern part of the Nyamulagira volcano, together with some localized deformation signals of about 1.5 cm/year located in the northern part of the Lake Kivu Province. Unfortunately, no coherent pixels have been detected in correspondence to the Nyiragongo active volcano, probably due to the presence of wide vegetated areas that strongly limit the possibility to extract reliable information about the occurred deformation (decorrelation phenomena).

**Table 5. Main characteristics of the exploited COSMO-SkyMed SAR data**

Orbit direction	Descending
Wavelength	3,1 cm
Acquisition mode	StripMap
Average look angle	~24°
Spatial resolution of the interferometric data	~30 m x 30 m
Time interval	13/04/2011 – 18/02/2019
Number of acquisitions	476
Number of interferograms	1479

**Table 6. Main characteristics of the exploited Sentinel-1 SAR data**

Orbit direction	Descending
Wavelength	5,5 cm
Acquisition mode	Terrain Observation by Progressive Scans
Average look angle	~39°
Spatial resolution of the interferometric data	~70 m x 70 m
Track	21
Time interval	10/06/2016 – 11/10/2019
Number of acquisitions	84
Number of interferograms	221

Thanks to the availability of C-band S-1 SAR acquisitions, characterized by a wider spatial extent (about 250 x 250 km<sup>2</sup>) with respect to the CSK frame, it has been possible to investigate a larger portion of the volcanic rift movement. In Figure 28 we show the LOS mean deformation velocity map of the S-1 data processing, superimposed on an optical image of the investigated area, relevant to the coherent pixels only. The S-1 mean deformation velocity map covers the same area highlighted by the CSK SBAS-DInSAR analysis, but extends North/East of the Nyamulagira volcano, including also the recent lava flows connected to the magma activity, characterized by an almost linear trend with rates up 3 cm/year.

Concerning the temporal evolution of the deformation, in Figure 29 we report the plots of the CSK and S-1 LOS-projected deformation time series (green triangles: CSK results, red triangles:

S-1 results) for four pixels, labeled as P1 to P4 and common to both SBAS-DInSAR datasets, which are characterized by significant deformation trends along the overall 2011-2019 time interval. The long term SBAS-DInSAR analysis performed with the CSK dataset allows us to detect also strong non linear deformation signals connected to the volcanic activity starting from the end of 2011, as clearly testified by the plot of the CSK deformation time series for pixel P1 (see Figure 29). Moreover, some non linear signals associated to localized deformation phenomena (lava flows, magma activities,...) in the southern part of the Nyamulagira volcano and in the northern part of the Lake Kivu Province are also clearly visible in the plots of the deformation time series for pixels P2-P4, although with different deformation rate changes occurring at different time epochs. The qualitative comparison of CSK and S-1 deformation time series with respect to the common time span shows a good agreement between the two series of DInSAR measurements.

Finally, we report in Figure 30 the plots of S-1 LOS-projected deformation time series for two pixels labeled as P5 and P6, located North/East of the Nyamulagira volcano (area not covered by the CSK analysis), characterized by an almost linear trend with rates up 3 cm/year.



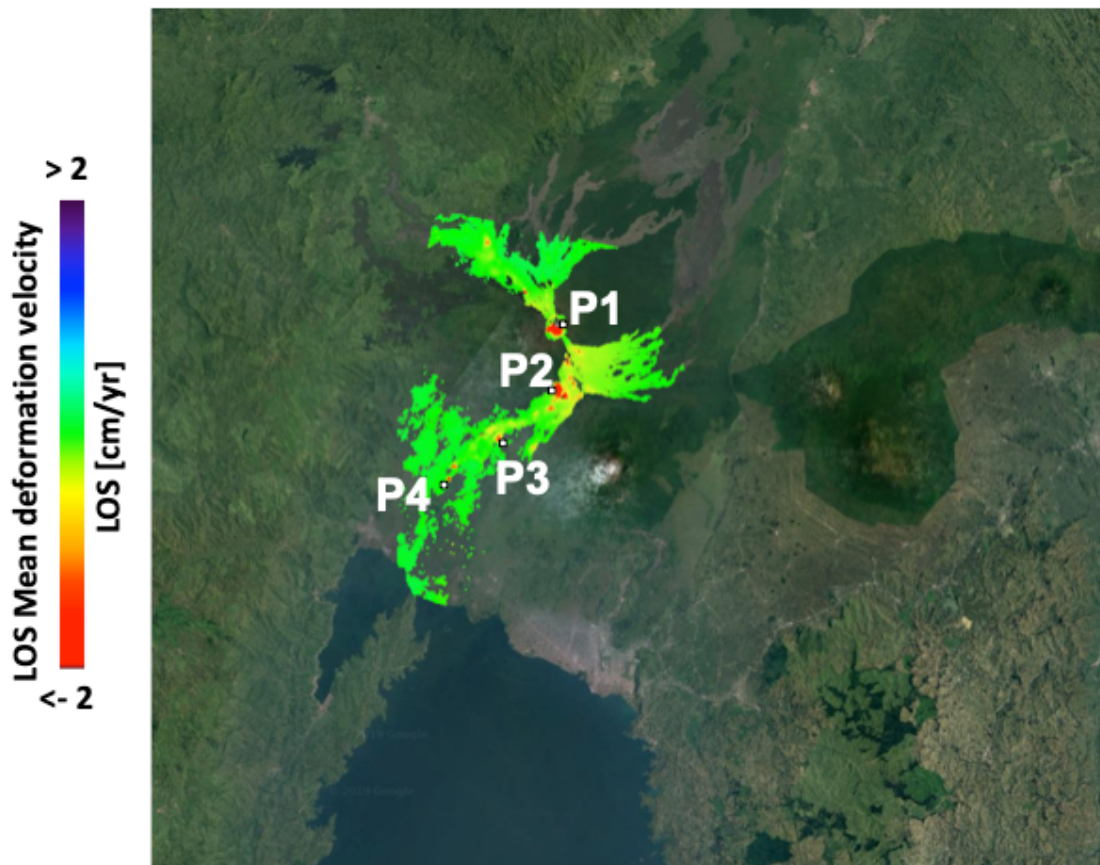


**Figure 27. LOS mean deformation velocity map (expressed in cm/year), geocoded and superimposed on an optical image of the investigated area. The results are relevant to the SBAS-DInSAR processing of the 2011-2019 CSK descending dataset. The location of four pixels (labeled as P1, P2, P3 and P4) characterized by significant deformation phenomena is here reported. The CSK deformation time series relevant to these four pixels are shown in Figure 29.**

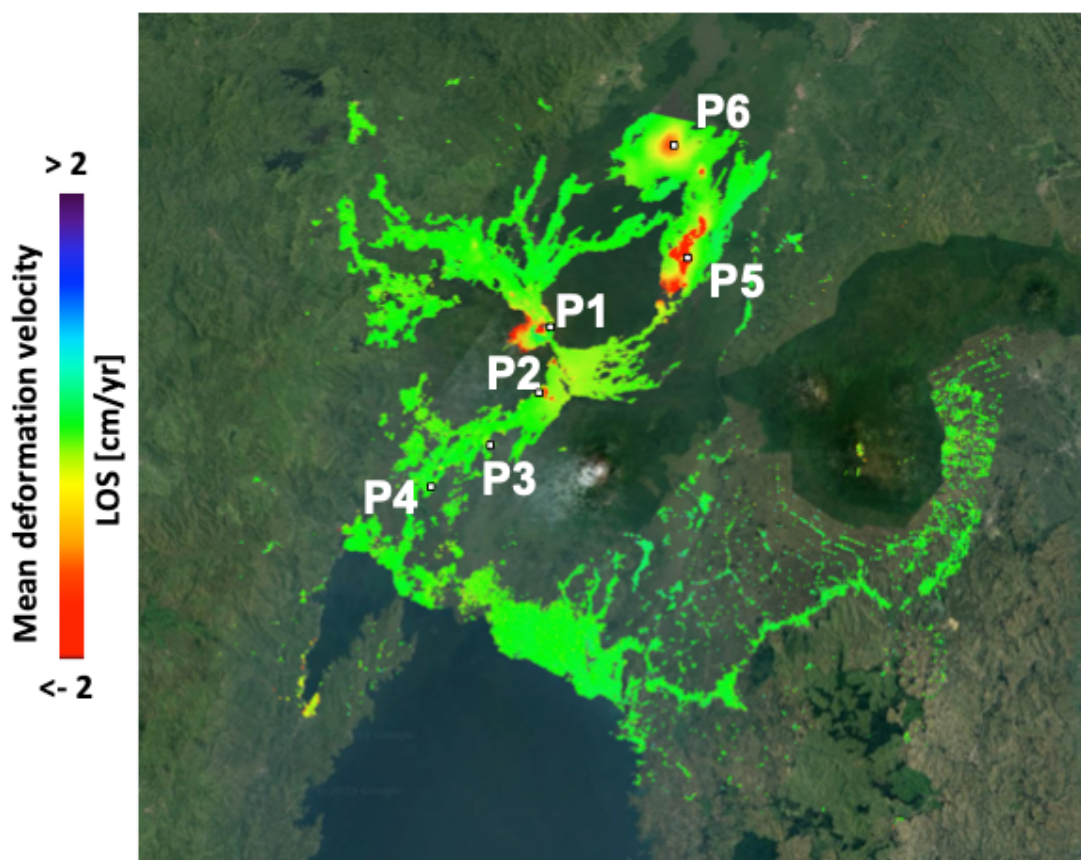


Figure 28. LOS mean deformation velocity map (expressed in cm/year), geocoded and superimposed on an optical image of the investigated area. The results are relevant to the SBAS-DInSAR processing of the 2016-2019 S-1 descending dataset. The location of 6 pixels (labeled as P1-P6), characterized by significant deformation phenomena is here reported. The S-1 deformation time series of pixels P1-P4, corresponding to the same pixels highlighted in Figure 27 for the CSK processing, are shown in Figure 29, whereas the S-1 deformation time series of P5 and P6 pixels are reported in Figure 30.

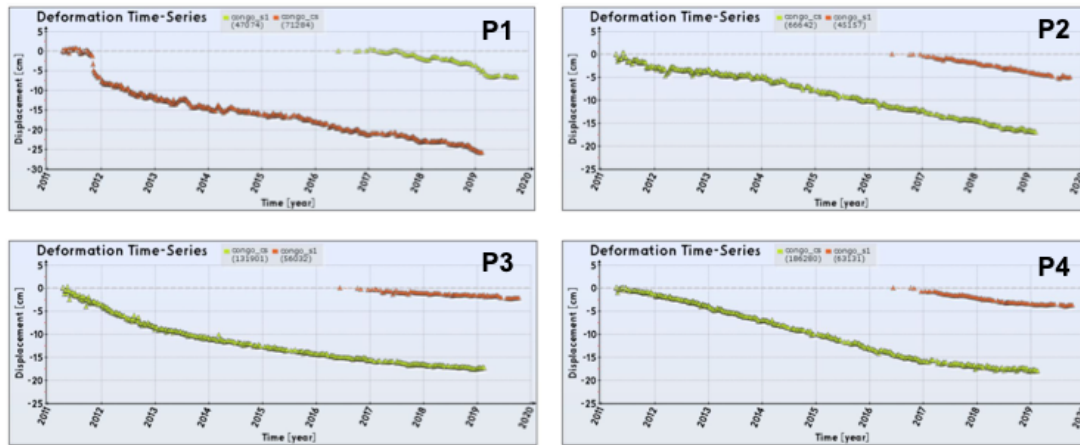


Figure 29. SBAS-DInSAR deformation time series: CSK (green triangles) and S-1 (red triangles) results for the P1-P4 pixels. The location of these pixels is reported in Figure 27 (CSK processing) and Figure 28 (S-1 processing).

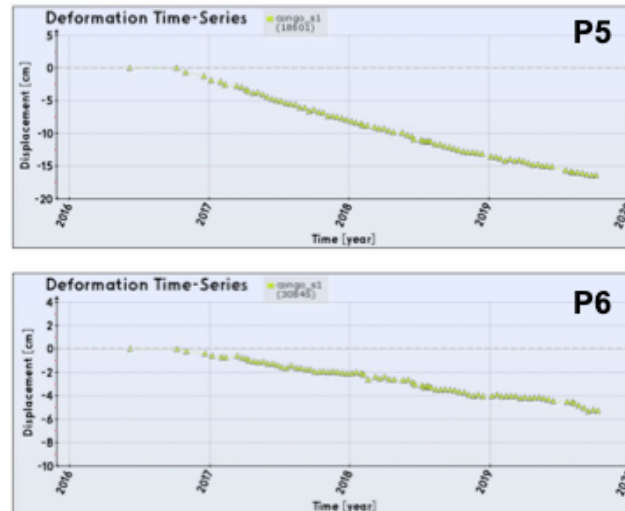
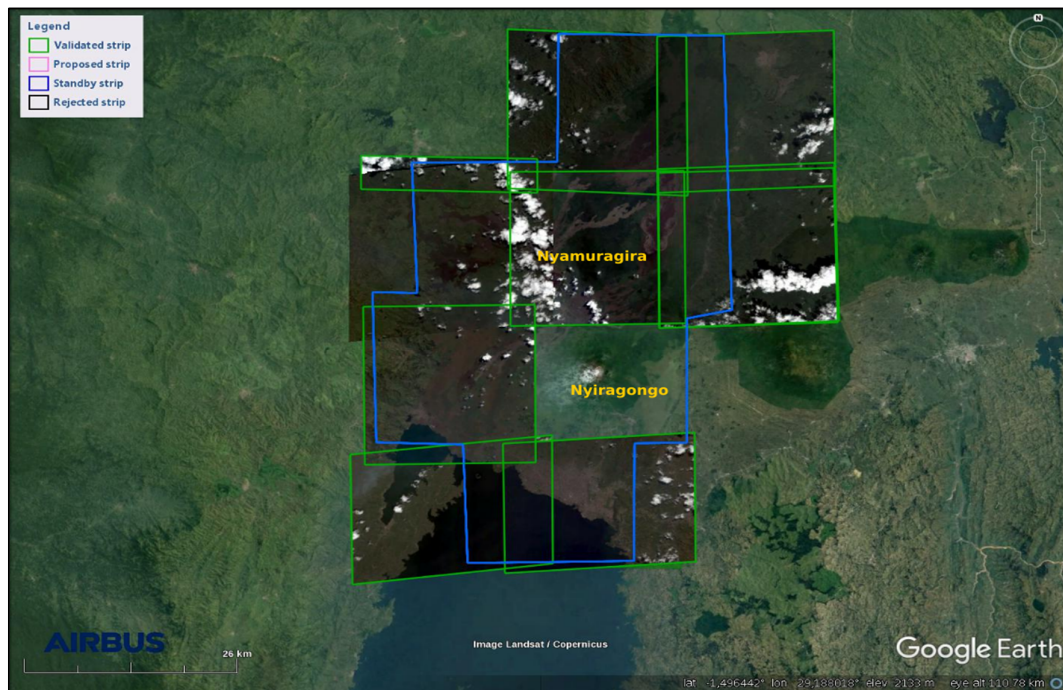


Figure 30. S-1 SBAS-DInSAR deformation time series for the pixels labeled as P5 and P6. The location of these pixels is reported in Figure 28.



### 5.2.2. Digital elevation model of the Virunga area from tri-stereo Pléiades data processing

In collaboration with the researchers of the Laboratory of Technologies for Volcanology (*TecnoLab*) at the INGV in Catania, the Virunga Volcanoes Supersite has produced a digital elevation model (DEM) of the Virunga area from high-resolution tri-stereo images acquired by the Pleiades satellites. The Pléiades constellation is composed by two optical satellites launched on December 2011 for Pléiades 1A and on December 2012 for Pléiades 1B, which provide images up to 50 cm spatial resolution that can be acquired in stereo and tri-stereo mode. From 26 December 2018 to 2 November 2019 different Pléiades acquisitions were performed on the Virunga area as shown in Figure 31.



**Figure 31.** Google Earth image of the Virunga area. The green boxes show the validated strips acquired during the period from December 2018 to November 2019. The area delimited by the blue line is the region of interest for the Pléiades data. The intersection between the two areas represents the Pléiades data available.

The Region of Interest (ROI, blue line) extends over an area of 2032 square kilometers. Of these, 1760 square kilometers were covered by the Pleiades acquisitions (green squares). It is worth notice that the Nyiragongo summit area is still missing and the Nyamulagira volcano is

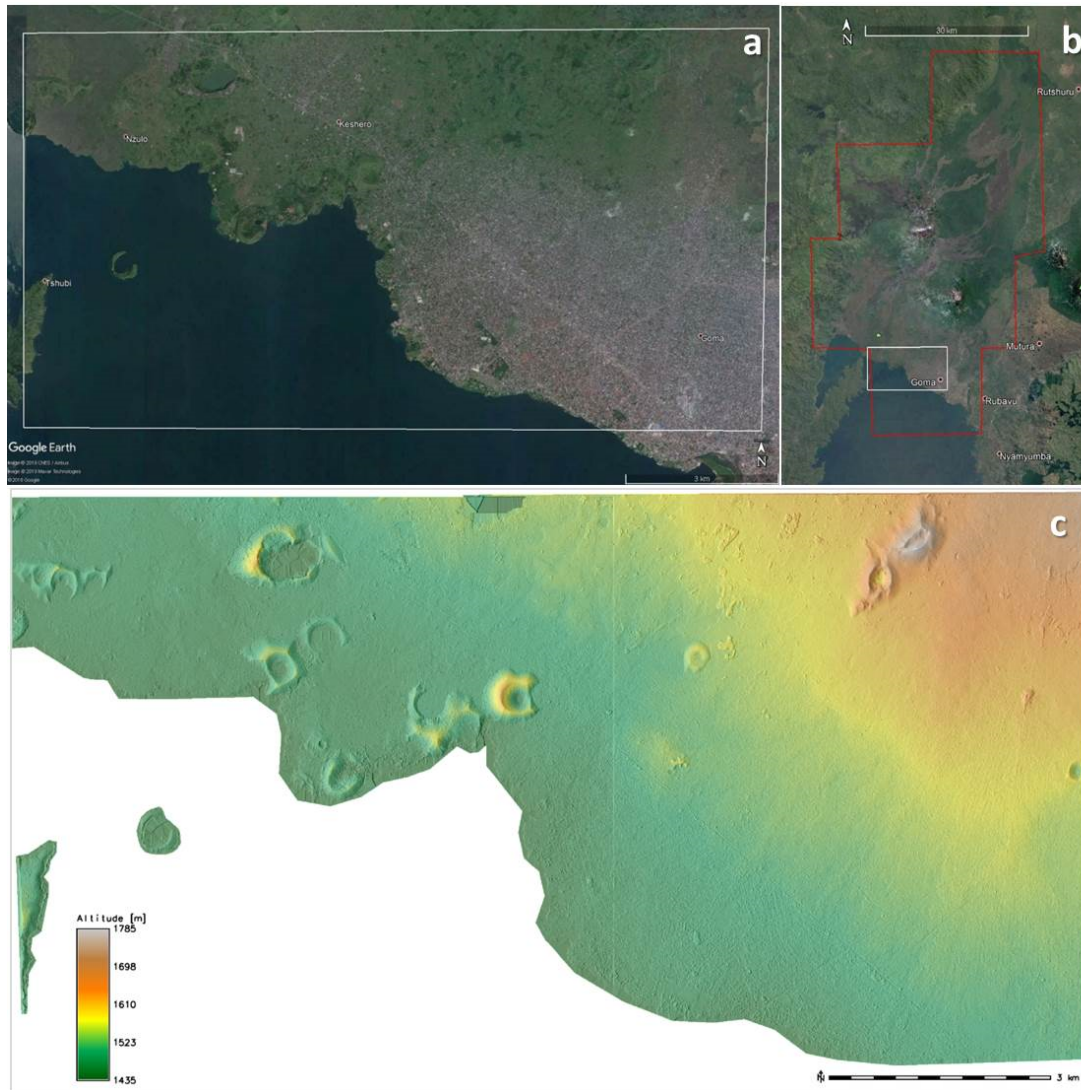
partially covered by clouds. Both issues will be solved during the upcoming acquisitions. The 3D processing of the tri-stereo Pléiades imagery was performed using the free and open source MicMac (Multi-images Correspondances, Méthodes Automatiques de Corrélation) photogrammetric library developed by the French Institut Géographique National [Rupnik et al., 2017]. MicMac is based on the principles of photogrammetry and consists of three main steps:

- 1) Tie points recognition and matching between images;
- 2) Calibration and orientation, recognizing relationships between view points and objects;
- 3) Correlation, producing dense matching for 3D scene reconstruction.

As result of this processing, a digital elevation model (DEM) composed by different patches was retrieved at the spatial resolution of 1 meter. Areas covered by clouds result necessarily in holes in the final product. The nominal absolute location accuracy of Pleiades-derived digital elevation model is 8.5 m [Oh and Lee, 2014], but this value is often an upper bound [Ganci et al., 2019]. Ground control points are required in order to evaluate the accuracy of the DEM in the Virunga area.

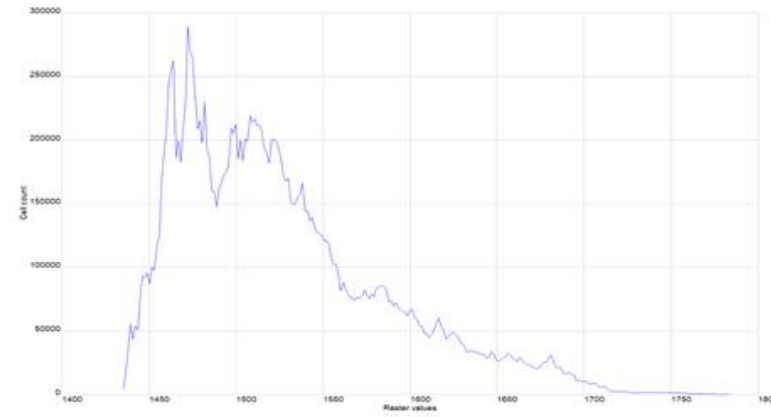
In the following, preliminary results in those areas with minimal impact from clouds are shown. All the elevation data were geocoded to the WGS84 UTM 35S reference coordinate system.





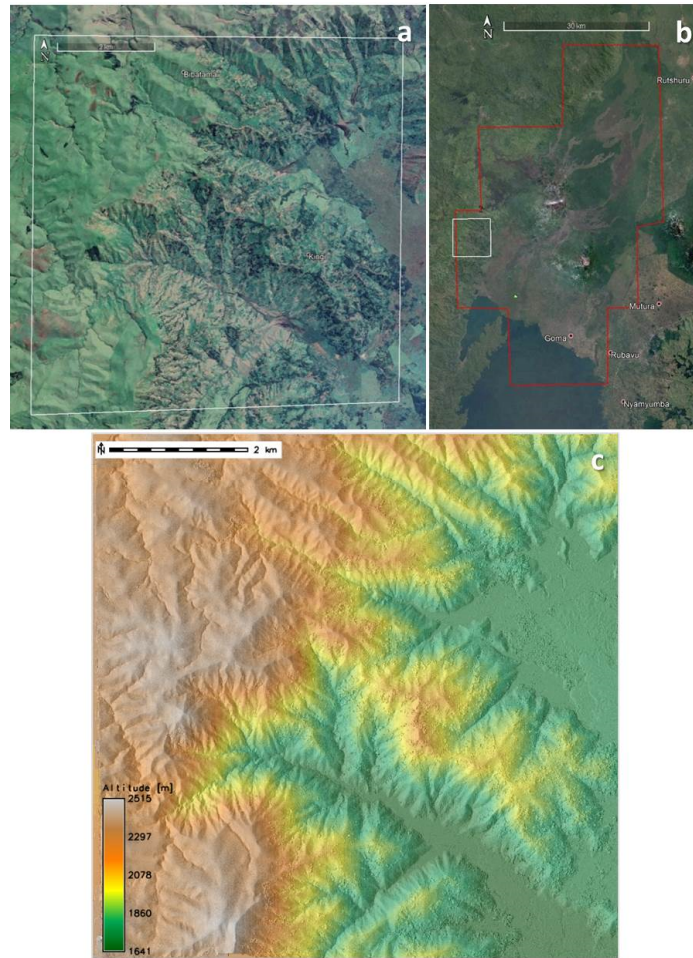
**Figure 32. a) Google earth map of the city of Goma. b) Location of the area with respect to the ROI. c) Shaded relief of the digital elevation model. Colors show the different altitudes.**

Figure 32 shows the resulting digital elevation model covering an area of 112.5 square kilometres including part of the city of Goma. Altitude values range between 1400 and 1780 meters. A plot with the frequency of each elevation is also reported in Figure 33.



**Figure 33. Elevation frequency for the DEM over the area of Goma.**

Figure 34 shows the resulting digital elevation model covering an area of 58 square kilometers including the mountainous area of Bibatama and Kingi. Altitude values range between 1640 and 2515 meters. A plot with the frequency of each elevation is also reported in Figure 35.



**Figure 34. Google earth map of the mountainous area of Bibatama and Kingi. b) Location of the area with respect to the ROI. c) Shaded relief of the digital elevation model. Colors show the different altitudes.**

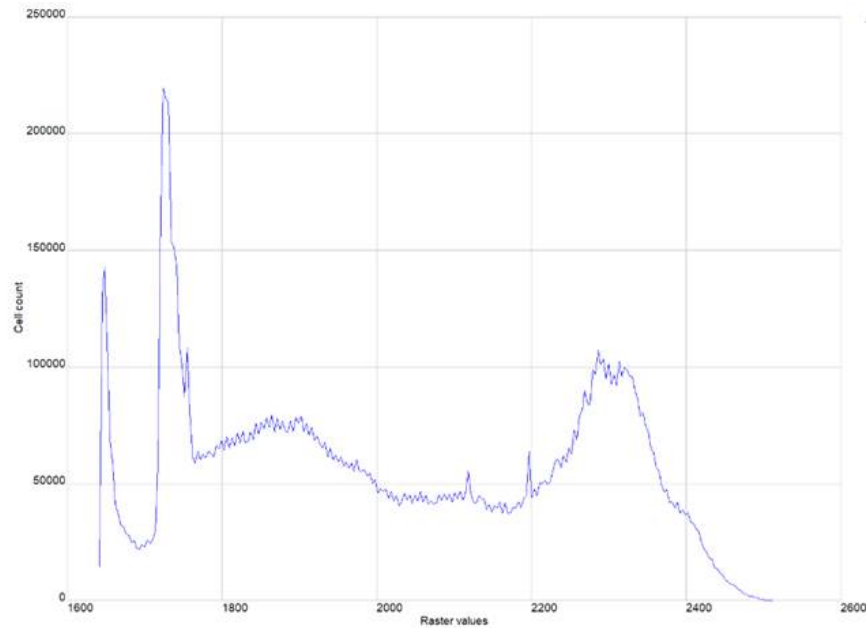


**Figure 35. Elevation frequency for the DEM over the areas of Bibatama and Kingi.**

Figure 36 shows the resulting digital elevation model covering an area of 64 square kilometers including the area of Lac Ondo. Altitude values range between 1027 and 1185 meters. A plot with the frequency of each elevation is also reported in Figure 37.



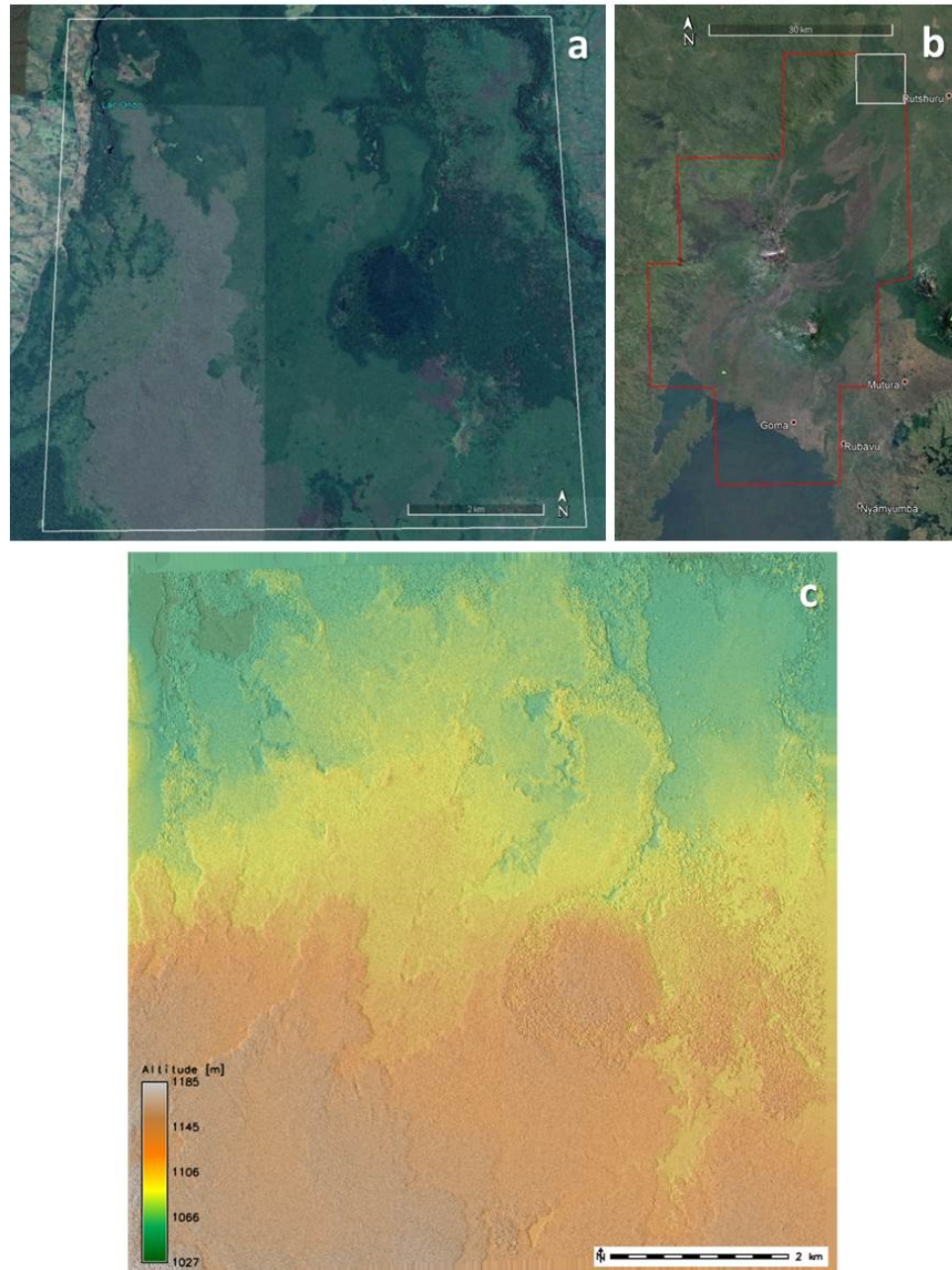


**Figure 36.** Google earth map of the area of Lac Ondo. b) Location of the area with respect to the ROI. c) Shaded relief of the digital elevation model. Colors show the different altitudes.



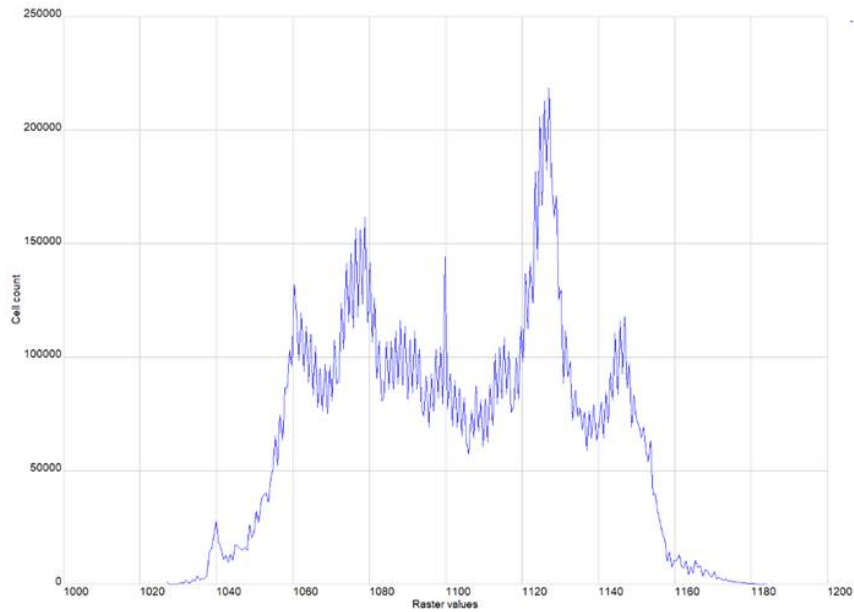


**Figure 37. Elevation frequency for the DEM over the area of Lac Ondo.**

### ***References:***

- Oh, J., and C. Lee (2014). Automated bias-compensation of rational polynomial coefficients of high resolution satellite imagery based on topographic maps, *ISPRS J. Photogramm. Remote Sens.*, 100, 12–22.
- Ganci, G., Cappello, A., Bilotta, G., Herault, A, Zago, V., Del Negro, C. (2018). Mapping Volcanic Deposits of the 2011–2015 Etna Eruptive Events Using Satellite Remote Sensing, vol. 6, 83, doi:10.3389/feart.2018.00083.
- Rupnik, E., Daakir, M., Pierrot Deseilligny, M. (2017). MicMac – a free, open-source solution for photogrammetry. *Open geospatial data, softw. stand.* 2: 14. doi:10.1186/s40965-017-0027-2.

### 5.2.3. Thermal activity at Nyiragongo and Nyamulagira detected by the MIROVA system

Below is summarized the satellite thermal observations made by the MIROVA system ([www.mirovaweb.it](http://www.mirovaweb.it)) on the Nyiragongo and Nyamulagira volcanoes.

**Nyiragongo volcano:** Since the January 17<sup>th</sup>, 2002 the MIROVA system has been detecting persistent thermal anomalies over Nyiragongo volcano, associated with the permanent lava lake activity inside the summit crater. On the whole 8315 thermal alerts have been detected until November 11<sup>th</sup> 2019, consisting in 1.28 thermal detection per day. The general trend recorded between 2002 and 2010 shows a gradual increase of Volcanic Radiative Power (VRP) increasing from 0 to ~ 1.5 GW, and punctuated by sporadic detections with VRP > 2 GW (Fig. 38a). This trend is likely associated to the rise of the lava lake level, accompanied by the gradual enlargement of the hot surface exposed to the atmosphere. Since 2010 the long-term thermal activity was more stable but with increasing episodes of monthly-long thermal pulses eventually producing short-live burst of thermal activity. These pulses become more frequent after 2016 (Fig. 38b). In Figure Fig. 38b, a detailed time series of VRP recorded between 2018 and 2020 shows the occurrence and the pattern of the two most recent thermal pulses occurred on July-August 2018 and March-April 2019, respectively. The highest thermal anomaly of the whole Nyiragongo dataset (2000-2020) occurred on April 2<sup>nd</sup> 2019 (at 19:55 UTC), when about 5 GW where recorded by MIROVA (Fig. 38b).

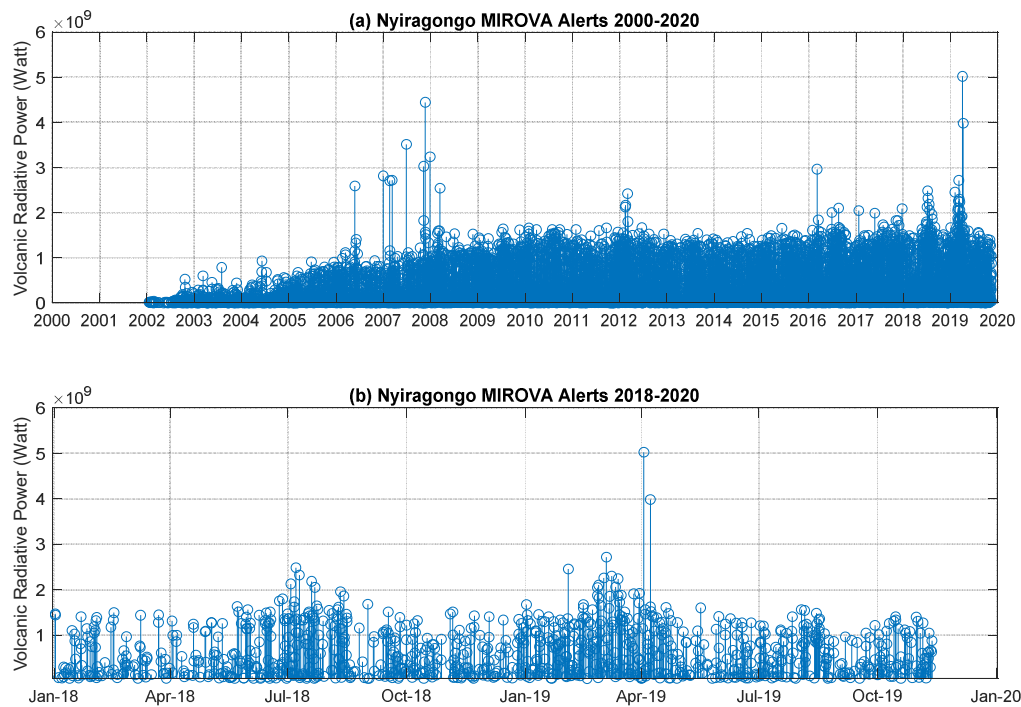


**Figure 38. Volcanic Radiative Power (VRP) recorded at Nyiragongo volcano by the MIROVA system. (a) Long-term thermal emission (2000-2020). (b) Thermal anomalies recorded between 2018 and 2020.**

**Nyamulagira volcano:** Between 2000 and 2020, the MIROVA system detected 2087 thermal alerts over Nyamulagira volcano. During the period 2000-2012 these anomalies were periodic, and exclusively associated to the flank effusive eruptions occurred in 2001 (February 6, 2001 to April 5, 2001), 2002 (July 25, 2002, then August 9, to September 27, 2002), 2004 (May 8, 2004 to May 28, 2004), 2006 (November 27, 2006 to December 5, 2006), 2010 (January 2, 2010 to January 27, 2010) and 2011-2012 (November 6, 2011 to mid-April, 2012), few small thermal anomalies recorded during intra-eruptive periods are associated to wild fires (Fig. 39a). This kind of effusive activity produced the highest thermal anomalies of the Nyamulagira dataset, with VRP typically reaching more than 1 GW (Fig. 2a; Coppola and Cigolini 2013). On the other hand, since 2014, lower but more persistent thermal anomalies were recorded on the summit of the volcano, likely associated to the birth and further evolution of a lava lake (Fig. 39b; Coppola et al., 2016b). In particular, all the VRP recorded after 2014 are essentially confined at the summit of the volcano and reach VRP lower than 1 GW. According to the thermal emission recorded by MIROVA, the lava lake activity inside the Nyamulagira crater shows at least three main phases on: Jan 2014 - March 2016, Jan – April 2017 and March 2018 – ongoing. Variable thermal activity recorded in each phase may represent phases of “rise and fall” of the lava lake level or eventually periods of major/minor lava effusion inside the summit pit-crater.

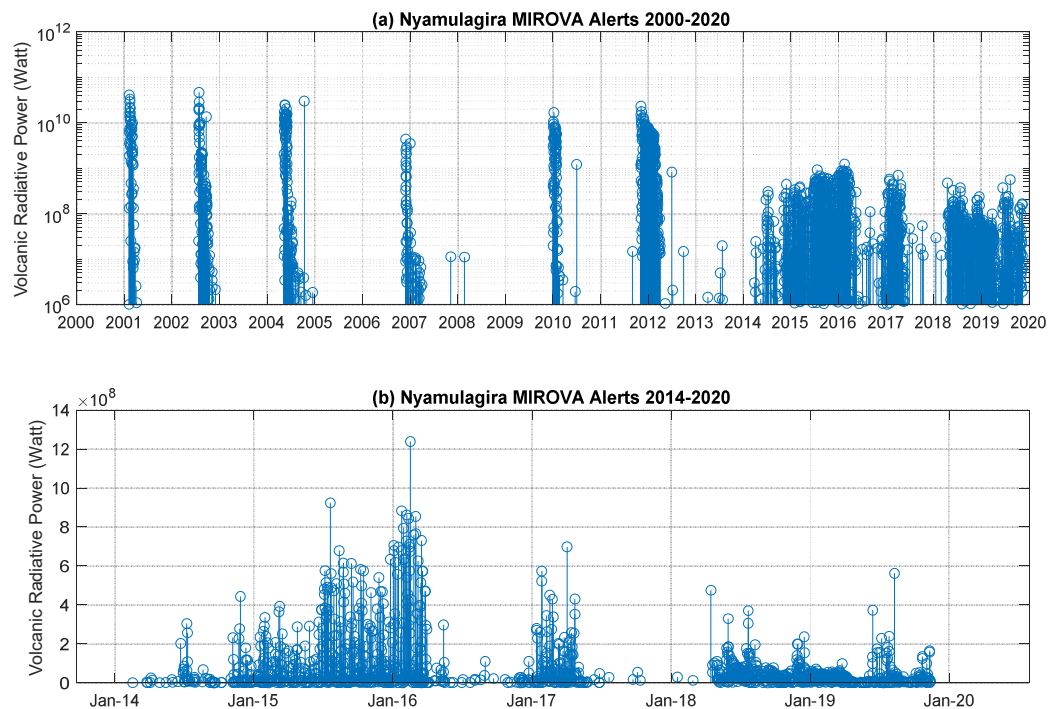


**Figure 39: Volcanic Radiative Power (VRP) recorded at Nyamulagira volcano by the MIROVA system. (a) Long-term (2000-2020) thermal emission in logarithmic scale. (b) Thermal anomalies recorded between 2014 and 2020.**

## References

- Balagizi, MC., Kies, A., Kasereka, M., Tedesco, D., Yalire, M., McCausland W., (2018) Natural hazards in Goma and the surrounding villages, East African Rift System. Springer's Journal of Natural Hazards, 93, 31–66,
- Balagizi, MC., Yalire, M., Ciraba, H., Kajeje, V., Minani, A., Kinja, A., Kasereka, M., (2016). Soil temperature and CO<sub>2</sub> degassing, SO<sub>2</sub> fluxes and field observations before and after the February 29, 2016 new vent inside Nyiragongo crater. Bulletin of Volcanology, 78 (9):1-11, <https://link.springer.com/article/10.1007/s00445-016-1055-y>
- Coppola, D., Laiolo, M., Cigolini, C., Delle Donne, D., Ripepe, M., (2016a). Enhanced volcanic hot-spot detection using MODIS IR data: results from the MIROVA system. In: Harris, A.J.L., De Groeve, T., Garel, F., Carn, S.A. (Eds.), Detecting, Modelling and Responding to Effusive Eruptions. Geological Society, London, Special Publications, vol. 426, p. 181-205. [dx.doi.org/10.1144/SP426.5](https://doi.org/10.1144/SP426.5).

Coppola, D., Campion, R., Laiolo, M., Cuoco, E., Balagizi, C., Ripepe, M., Cigolini, C., Tedesco, D. (2016b). Birth of a lava lake: Nyamulagira volcano 2011-2015. *Bulletin of Volcanology*, vol. 78(3), p. 1-13. doi: 10.1007/s00445-016-1014-7.

Coppola D., Cigolini C. (2013). Thermal regimes and effusive trends at Nyamuragira volcano (DRC) from MODIS infrared data. *Bulletin of Volcanology*, vol. 75(8), p. 1-15, doi: 10.1007/s00445-013-0744-z.

## Publications

### Peer reviewed journal articles

- Tuluka, G.M., Lukindula, J. & Durrheim., R. (2019). Seismic Hazard Assessment of the Democratic Republic of Congo and Environs Based on the GEM–SSA Catalogue and a New Seismic Source Model *Journal of Pure and Applied Geophysics*. doi.org/10.1007/s00024-018-2084-6
- Balagizi, C., and Liotta, M. (2019). Key factors of precipitation stable isotope fractionation in Central-Eastern Africa and Central Mediterranean. *Geosciences* 2019, 9.
- Balagizi, C., Kies, A., Kasereka, M., Tedesco, D., Yalire, M., McCausland, W. A. (2018). Natural hazards in Goma and the surrounding villages, East African Rift System. *Springer's Journal of Natural Hazards*, 93, 31–66, <https://doi.org/10.1007/s11069-018-3288-x>
- Balagizi, M., Kasereka, M., Cuoco, E., Liotta, M. (2018). Influence of moisture source dynamics and weather patterns on stable isotopes ratios of precipitation in Central-Eastern Africa. *Science of the Total Environment Journal*, 628 (629C), 1058-1078, <https://doi.org/10.1016/j.scitotenv.2018.01.284>
- Kasereka, M., Yalire, M., Minani, A. S., Samba, C. V., Bisusa, A. K., Kamate, E. K., Mashagiro, N., Syaushwa, M., Kavuke, J. K. (2017). Risks Associated with Mazuku in the Goma area, Democratic Republic of the Congo (East African Rift). *J. Wat. Env. Sci. Vol. 1*, 164-174.
- Balagizi, M., Kasereka, M., Cuoco, E., Liotta, M. (2017). Rain-plume interactions at Nyiragongo and Nyamulagira volcanoes and associated rainwater hazards, East Africa, *Applied Geochemistry* 81 (2017) 76-89 ; <http://dx.doi.org/10.1016/j.apgeochem.2017.03.018>

### Conference presentations/proceedings

- Balagizi (2019). Challenges for setting up a reliable volcanic risk reduction program in less developed countries: the case of the Goma Volcano Observatory, DR Congo. *VOLCANO OBSERVATORY BEST PRACTICES WORKSHOP #4*, 18-23 November 2019, Mexico City.
- Balagizi (2019) Impacts of Virunga active volcanism on water chemistry, East African Rift. May 13<sup>th</sup>, 2019. Helmholtz Centre for Environmental Research – UFZ, Lake physics and Lake Modelling Unit; Magdeburg- Germany
- Balagizi (2019) Characteristics of Water Geochemistry in the Virunga, a young active volcanic and continental rift zone. May 7<sup>th</sup>, 2019. Institut für Geologie; Universität Hamburg - Germany
- Balagizi (2019) Characteristics of Water Geochemistry in the Virunga, a young active volcanic and continental rift zone. May 7<sup>th</sup>, 2019. Institut für Geologie; Universität Hamburg - Germany <https://www.geo.uni-hamburg.de/geologie/ueber-das-institut/nachrichtenaufstellung/biogeochemical-seminar-07052019.html>
- Balagizi, C., Kasereka, M., Cuoco, E., Liotta, M. (2019) Environmental and health impacts of Nyiragongo and Nyamulagira Volcanoes, East Africa. *Geophysical Research Abstracts*, Vol. 21, EGU2019-5695, 2019. European Geosciences Union General Assembly 2019, Vienna-Austria
- Balagizi, C., Kies, A., Kasereka, M., Tedesco, D., Yalire, M., McCausland, W. A. (2018). Natural hazards in Goma and the surrounding villages, East African Rift System. In *Scenario-based hazard and risk assessment Development and application for volcanic risk management. Cities on Volcanoes conference*, September 2-7, Naples-Italy. <http://www.ingv.it/editoria/miscellanea/2018/miscellanea43/> (see page 1001)



**Balagizi C. and Virunga Supersite supporting scientists and agencies (2018) Virunga Supersite: implementation status, preliminary results and future challenges. The role of the GEO-GSNL initiative and of integrated research infrastructures in improving the knowledge of volcano dynamics and hazard. Cities on Volcanoes conference, September 2-7, Naples- Italy.**  
<http://www.ingv.it/editoria/miscellanea/2018/miscellanea43/> (see page 863)

**Balagizi, C., Mahinda, C., Yalire, M., Ciraba, H., and Tuluka, G. (2017). Geophysical Research Abstracts, Vol. 19, EGU2017-3237, 23-28, Vienna - Austria**

NOTE: Here we only list the conference presentations and proceedings gave by the Supersite coordinator for the promotion of the Supersite in Universities and research centers, and for discussing and disseminating the Supersite results and work plan the in conferences and workshops.

### Research products

Type of product	Product provider	How to access	Type of access
<b>SSA Catalogue and a New Seismic Source Model</b>	Mavonga, G, Lukindula, J. and Durrheim, J	<a href="https://link.springer.com/article/10.1007/s00024-018-2084-6">https://link.springer.com/article/10.1007/s00024-018-2084-6</a>	Publication
<b>Maps of Mazuku and fractures in Goma</b>	Balagizi, C., Kies, A., Kasereka, M., Tedesco, D., Yalire, M., and McCausland, W. A.	<a href="https://link.springer.com/article/10.1007/s11069-018-3288-x">https://link.springer.com/article/10.1007/s11069-018-3288-x</a>	Publication
<b>Goma City: Transportation Network Vulnerability to Nyiragongo's lava flow Map - Volcanic Risk Assessment (Overview)</b>	Copernicus-Emergency Management Service – Mapping and Goma Volcano Observatory (GVO)	<a href="https://emergency.copernicus.eu/mapping/list-of-components/EMSN047">https://emergency.copernicus.eu/mapping/list-of-components/EMSN047</a>	Public
<b>Goma city: Lava Flow Hazard Map - Volcanic Risk Assessment (Overview)</b>	Copernicus-Emergency Management Service – Mapping and GVO	<a href="https://emergency.copernicus.eu/mapping/list-of-components/EMSN047">https://emergency.copernicus.eu/mapping/list-of-components/EMSN047</a>	Public
<b>Goma city and surrounding: Land Use and Land Cover Map - Volcanic Risk Assessment</b>	Copernicus-Emergency Management Service – Mapping and GVO	<a href="https://emergency.copernicus.eu/mapping/list-of-components/EMSN047">https://emergency.copernicus.eu/mapping/list-of-components/EMSN047</a>	Public
<b>Goma city: Reference Map - Volcanic Risk Assessment (Overview)</b>	Copernicus-Emergency Management Service – Mapping and GVO	<a href="https://emergency.copernicus.eu/mapping/list-of-components/EMSN047">https://emergency.copernicus.eu/mapping/list-of-components/EMSN047</a>	Public
<b>Digital Elevation Model (5m resolution on ground)</b>	Copernicus-Emergency Management Service – Mapping and GVO	<a href="https://emergency.copernicus.eu/mapping/list-of-components/EMSN047">https://emergency.copernicus.eu/mapping/list-of-components/EMSN047</a>	Public

NOTE: Other products are not ready yet, the work is ongoing; Interferogram, improved VHR DEM, improved Hazards maps where more ground-based data are being inserted.

### Research product issues

The research products are open to other scientists and to the public but the language limitation is a major issue for both the local stakeholders and population. The other concern is that the products are available online while locally internet is not accessible for the majority of the population.

As future development, the research products have to be translated in local language(s), e.g. each important finding published in scientific papers could be summarized in local language(s) and hazards maps shall have version with maps information is in local language(s). Moreover, some products will need to be both in local language(s) and provided in printed version and then available to stakeholders and local public.

## 6. Dissemination and outreach

- All the scientific products a particularly the hazards maps are delivered (download links are provided and data hand given through key drivers) to the staff of the Goma Observatory which then delivers them to the the Conseil Provincial de prévention des catastrophes au Nord-Kivu, in D.R.C. (Provincial Council for Disaster Reduction). This council includes the national Civil Protection, the Congolese Red Cross, the Ministries of Interior, Urbanism and research. The products were also delivered to similar institutions in Rwanda, where the risk from a Nyiragongo eruption is also very high.
- The Virunga Volcanoes Supersite initiative and results have been presented in seminars at universities and research centers, in formal meetings and workshops at both local and international levels to first let them know of the existence of the Supersite, show the scientific opportunities to being member of this community, and then bring them contribute to the activities of the Supersite.
- The scientific products as well as any EO data made available have been emailed to the each of the Virunga Scientific community, and the products made available online, shared through social medias,...

## 7. Funding

- The Virunga Volcanoes Supersite has no funds and has not been involved in any projects; all the activities were realized by scientists on a voluntary basis. However, and as already mentioned, some activities that required funding (e.g. short trainings, the attendance to meetings and workshops) have benefited from the support from INGV, the USGS-VDAP, the Volcano Active foundation, the IAVCEI.
- A project proposal has been written in collaboration with Virunga Volcanoes Supersite Core Team scientists, the requested funding is to help the supersite reach its key goals

such as long-term trainings abroad for local scientists, support international scientists come to Goma for short trainings and common field works with the local scientists, acquisition of infrastructures and equipment for ground-based data collection, and data processing in general.

## 8. Stakeholders interaction and societal benefits

The Goma Volcano Observatory is the first beneficiary of the Virunga Supersite services and products when considering its mission of studying and monitoring Virunga volcanoes, and of providing key information to all others governmental and non-governmental agencies involved in risk management at both national and regional levels. This justifies the important interactions that exist between the Supersite and the Observatory, and also considering the fact that the GVO is in charge of producing the types of information the Supersite is providing, and is the institution able to use other products from the Supersite such as the Earth Observation data, or mostly in need of services such as the training of researchers and technicians. Furthermore, based on local organization, the GVO is the specialized organization that provides products to other services such as the hazards maps, and their dissemination among stakeholders in general and particularly to the population.

Hence, though the GVO the products were delivered to the stakeholders (Nord-Kivu's Provincial Council for Disaster Reduction, Nord-Kivu Civil Protection, the Congolese Red Cross, UN mission in Congo, the NGOs and the Ministries of the Interior, Urbanism and research. The products were also delivered to similar institutions in the neighboring republic of Rwanda. These "ready to use" products and that have direct societal benefits include (1) the Seismic Hazard Assessment of the Democratic Republic of Congo and Environs discussed in section 5.1.1., (2) the map fractures in Goma city (Figure 4), (3) the map of the location of Mazuku with CO<sub>2</sub> concentration range from 20 to 71% (Figure 6), (4) the vertical profiles of fluoride concentration in the main basin of Lake Kivu and Kabuno Bay (Figure 8A, note that tap water distributed in Goma is pumped from Lake Kivu), (5) the fluoride concentration in the rivers and rainwaters around Nyiragongo and Nyamulagira volcanoes where these waters are used for drinking (Figure 8), (6) the reference map that includes topographic elements, settlements, transport network, POIs, etc. (Figure 21), (8) the land use and cover mapping (Figure 22), the Very High Digital Elevation image, (9) the lava Flow Hazard map and Exposure of assets and population (Figure 23), and (10) the Road Network Vulnerability to lava flow (Figure 24) very useful for volcano eruption crisis.

## 9. Conclusive remarks and suggestions for improvement

The Virunga Volcanoes Supersite has brought together a large number of top-level scientists and agencies to support the study and monitoring of Africa's most active and dangerous volcanoes. Building such a voluntary scientific team working with space agencies providing EO

data free of charge to support the improvement of geophysical scientific research and geohazard assessment, and thus enhanced societal benefits in DRR in an area with important scientific problems and high-risk levels is the fundament of the GSNL. Thus, one of the success of the Virunga Volcanoes Supersite is that it has materialized this concept, which has generated the products listed in section 8 and detailed in sections 5.1. and 5.2. related to in situ and satellite research results, respectively. The Virunga Supersite has therefore been a great success. As already mentioned, the generated research results are crucial products as they are associated to with pre-crisis assessment of hazards in the region, support ongoing monitoring activities, disaster and crisis preparedness and management.

The Virunga Supersite has encountered several issues of which the important are listed below:

- **Issue related to in situ data:** we are in a strong need to enlarge and improve the existing in situ data collection networks and activities, are therefore searching equipment to deploy in the field.
- **Issue related to Satellite data:** The provision of COSMO-SkyMed data has been very good but are still provided as archived data. We need to receive new in a near real time mode over the two active volcanoes to support the monitoring activities. We have requested from ASI to move the quota budget allocated in 2019 to new acquisitions (100 images over Virunga Volcano and 100 images over the Kivu Lake) for the current year 2020, which means that a total amount of 400 images should be provided during this year. Since eruptions at Nyiragongo and Nyamulagira are initiated by the rift opening movements, both shallow and deep fractures in the field of active volcanoes will be identified, mapped and later monitored using these COSMO-SkyMed data. Furthermore, the ground deformation related to the changes in the level of volcanic activity will be monitored in order to capture any rising movements of the magma towards the surface, which is a key parameter to predict possible future eruption events and vents. Moreover, since in the region high levels of earthquake and landslide hazards also exist, the CSK data will be further used to generate deformation time series. This will allow to identify and map the location of normal and non-normal faults in correspondence to the northern and southern Lake Kivu Basin, whose activities are linked to that of the rift and along which the major impacts of past earthquake events have been located so far.

Regarding the Pleiades images in the Virunga region, there is a big issue of clouds affecting the quality of the images. We have suggested that second redundancy acquisitions are should be planned to obtain the complete coverage which are free of clouds. We therefore request that these second redundancy acquisitions to not be included in the yearly quota of the images to be delivered to the Supersite by the CNES.

- **infrastructures and capacity development of local scientists.**

Some of the important goals of the Virunga Volcanoes Supersite are in relation with solving the issues related to situ data collection by acquiring the necessary equipment, support infrastructures and capacity development of local scientists. Even though the mission of the GSNL is not to providing funds to the Supersites, there is however expectations that the established Supersite for further develop of local structural and scientific capacities through the increased collaboration and international visibility offered by the GSNL and the COES

networks. Thus, we kindly request from the GSNL and COES to support raise funds by helping contact potential funders to whom a project proposal could be submitted.